2055

VTT RESEARCH NOTES

VTT TIEDOTTEITA

**Pekka Stén, Markus Olin & Jarmo Lehikoinen**

# Surface complexation on iron oxides with reference to the oxide films formed on material surfaces in nuclear power plants

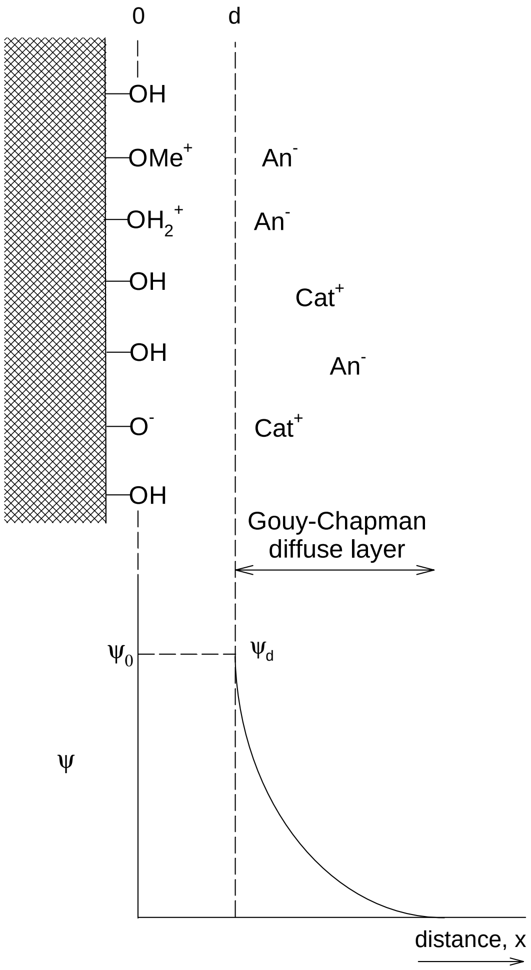

TECHNICAL RESEARCH CENTRE OF FINLAND

ESPOO 2000

VTT TIEDOTTEITA – MEDDELANDEN – RESEARCH NOTES 2055

# Surface complexation on iron oxides with reference to the oxide films formed on material surfaces in nuclear power plants

Pekka Stén, Markus Olin & Jarmo Lehikoinen
VTT Chemical Technology

TECHNICAL RESEARCH CENTRE OF FINLAND
ESPOO 2000

ISBN 951–38– 5749–2 (nid.)
ISSN 1235–0605 (nid.)

ISBN 951–38–5752–2 (URL: http://www.inf.vtt.fi/pdf/)
ISSN 1455–0865 (URL: http://www.inf.vtt.fi/pdf/)

JULKAISIJA – UTGIVARE – PUBLISHER

Valtion teknillinen tutkimuskeskus (VTT), Vuorimiehentie 5, PL 2000, 02044 VTT
puh. vaihde (09) 4561, faksi (09) 456 4374

Statens tekniska forskningscentral (VTT), Bergsmansvägen 5, PB 2000, 02044 VTT
tel. växel (09) 4561, fax (09) 456 4374

Technical Research Centre of Finland (VTT), Vuorimiehentie 5, P.O.Box 2000, FIN–02044 VTT, Finland
phone internat. + 358 9 4561, fax + 358 9 456 4374

VTT Kemiantekniikka, Mineraalitekniikka, Tutkijankatu 1, PL 1405, 83501 OUTOKUMPU
puh. vaihde (013) 5571, faksi (013) 557 557

VTT Kemiteknik, Mineralteknik, Tutkijankatu 1, PB 1405, 83501 OUTOKUMPU
tel. växel (013) 5571, fax (013) 557 557

VTT Chemical Technology, Mineral Processing,
Tutkijankatu 1, P.O.Box 1405, FIN–83501 OUTOKUMPU, Finland
phone internat. + 358 13 5571, fax + 358 13 557 557

VTT Kemiantekniikka, Ympäristötekniikka, Betonimiehenkuja 5, PL 14032, 02044 VTT
puh. vaihde (09) 4561, faksi (09) 456 7043

VTT Kemiteknik, Miljöteknik, Betongblandargränden 5, PB 14032, 02044 VTT
tel. växel (09) 4561, fax (09) 456 7043

VTT Chemical Technology, Environmental Technology,
Betonimiehenkuja 5, PL 14032, FIN–02044 VTT, Finland
phone internat. + 358 9 4561, fax + 358 9 456 7043

VTT Kemiantekniikka, Teollisuusfysiikka, Otakaari 3 A, PL 1404, 02044 VTT
puh. vaihde (09) 4561, faksi (09) 456 6390

VTT Kemiteknik, Industrifysik, Otsvängen 3 A, PB 1404, 02044 VTT
tel. växel (09) 4561, fax (09) 456 6390

VTT Chemical Technology, Industrial Physics, Otakaari 3 A, P.O.Box 1404, FIN–02044 VTT, Finland
phone internat. + 358 9 4561, fax + 358 9 456 6390

Technical editing Maini Manninen

Text preparing Tarja Haapalainen

Otamedia Oy, Espoo 2000

Stén, Pekka, Olin, Markus & Lehikoinen, Jarmo. Surface complexation on iron oxides with reference to the oxide films formed on material surfaces in nuclear power plants. Espoo 2000, Technical Research Centre of Finland, VTT Tiedotteita – Meddelanden – Research Notes 2055. 70 p.

**Keywords** nuclear power plants, adsorption, surface complexation, iron oxides, oxide films, ferrihydrite, hydrous ferric oxide, zinc, cobalt

# Abstract

The construction materials used in coolant systems in nuclear power plants become covered with oxide films as a result of exposure to the aqueous coolant. The present work belongs to a research programme on the properties of such films and especially on the transport of inorganic species through the films. The focus is on the incorporation of the highly energetic long-lived cobalt isotope $^{60}$Co in the films causing build-up of radiation fields in the out-of-core system.

The first step in $^{60}$Co incorporation in the oxide films on the primary circuit surfaces is assumed to be adsorption which can be modelled using the surface complexation approach. The review begins with a general discussion of surface complexation on various iron oxides. After introducing the main concepts of surface complexation modelling, three of the most common models (the constant capacitance model, the diffuse layer model and the triple layer model) are discussed and compared.

The very outermost layer of the oxide film is assumed to be more or less hydrated and poorly ordered resembling ferrihydrite known also as hydrous ferric oxide. Consequently, the surface chemical properties of and adsorption on ferrihydrite are reviewed. Using the known and estimated physical properties of the cooling system, chemical composition of the coolant and literature data on the surface and solution reactions, equilibrium calculations are conducted by the HYDRAQL programme to predict adsorption behaviour of cobalt and zinc on ferrihydrite at 25 °C. Except temperature, the conditions simulated in these calculations are similar to those prevailing in the cooling systems. The calculations correctly predict the diminishing effect of zinc on cobalt adsorption.

The published surface complexation studies on iron oxides at elevated temperatures are reviewed. Despite the importance of the temperature on adsorption, surface complexation studies at other than room temperature are rare and the high-temperature, high-pressure regime is almost unexplored. The few studies found in the literature indicate that at the elevated temperatures, the charging of the oxide surface will play a much more significant role in the adsorption of ions than at room temperature. Increasing the temperature of the system is known to promote significantly cation uptake. Another general trend is the decrease of the point of zero charge of oxides with increasing temperature.

Stén, Pekka, Olin, Markus & Lehikoinen, Jarmo. Surface complexation on iron oxides with reference to the oxide films formed on material surfaces in nuclear power plants. Espoo 2000, Technical Research Centre of Finland, VTT Tiedotteita – Meddelanden – Research Notes 2055. 70 p.

**Keywords** nuclear power plants, adsorption, surface complexation, iron oxides, oxide films, ferrihydrite, hydrous ferric oxide, zinc, cobalt

# Tiivistelmä

Ydinvoimalaitosten jäähdytysvesipiirien putkistoissa käytettävien rakennemateriaalien pinnoille syntyy veden hapettavan vaikutuksen vuoksi hapettumakerros eli oksidifilmi. Tämä työ on osa näiden oksidifilmien ominaisuuksiin keskittyvää laajempaa tutkimuskokonaisuutta. Erityisen mielenkiinnon kohteena on radioaktiivisen koboltti-60-isotoopin joutuminen filmeihin, mikä aiheuttaa aktiivisuuden kerääntymistä primääripiirin pinnoille.

Tässä julkaisussa esitettävä tarkastelu perustuu oletukseen, jonka mukaan adsorptio filmi-jäähdytysvesirajapinnalla on ensimmäinen vaihe $^{60}$Co-isotoopin joutumisessa filmiin. Adsorptiota oksidipinnoille on 1970-luvulta lähtien kuvattu ns. pintakompleksaatiomallien avulla. Julkaisun alussa esitetään pintakompleksaatiomallinnuksen yleiset perusteet ja verrataan kolmea näissä malleissa tavallisimmin käytettyä tapaa kuvata ionisten osaslajien adsorptioon liittyvät sähköstaattiset vuorovaikutukset kiintoaine-liuosrajapinnoilla.

Rakennemateriaalien pinnoille korkealämpötilavedessä muodostuvien filmien uloimman kerroksen oletetaan tässä tarkastelussa muistuttavan huonosti kiteytynyttä raudan oksidia, ferrihydriittiä. Julkaisuun on koottu katsaus kirjallisuudessa esitetyistä ferrihydriitin pintakemiallisista ominaisuuksista sekä koboltin ja sinkin adsorptiota käsittelevistä tutkimuksista. Kirjallisuudesta haettujen pinta- ja liuosreaktioiden tasapainovakioiden sekä jäähdytysveden koostumuksesta ja järjestelmän fysikaalisista ominaisuuksista käytettävissä olevien tietojen perusteella on arvioitu sinkin ja koboltin adsorptiota oksidifilmeille. Laskut on tehty käyttäen HYDRAQL-ohjelmaa, jolla simuloidut olot lämpötilaa (25 °C) lukuun ottamatta, muistuttavat jäähdytysvesipiirien oloja. Laskentamalli ennustaa käytännössäkin havaitun jäähdytysveteen tapahtuvan sinkin lisäämisen koboltin adsorptiota vähentävän edullisen vaikutuksen.

Tärkeydestään huolimatta lämpötilan vaikutusta pintakompleksaatioon on tutkittu vain vähän. Korkealämpötilaoloissa (>100 °C) tutkimuksia on tehty vasta aivan viime vuosina ainoan tutkitun rautaoksidin ollessa magnetiitti. Lämpötilan vaikutus pintakompleksaatioon on kuitenkin merkittävä kationien adsorption kasvaessa huomattavasti lämpötilan noustessa. Toinen yleinen piirre on oksidien pinnan nollavarausta vastaavan pH:n pieneneminen lämpötilan kasvaessa.

# Contents

# 1. Introduction

In the operation of water-cooled nuclear reactors, the increase of radioactivity in the out-of-core system, e.g. piping, is a serious problem. The radioactive contamination is mainly due to the highly energetic long-lived cobalt isotope $^{60}$Co. Natural cobalt isotope, $^{59}$Co, is introduced in nuclear reactors both as an impurity of constituent steels and as major constituent of special alloys such as Stellite. The interaction between the construction materials and the aqueous coolant leads to the formation of oxide films on the piping surfaces and to the release of small amounts of metals, e.g. $^{59}$Co, into the coolant. The released cobalt is carried by this coolant into the core of the nuclear reactor where the $^{60}$Co isotope is formed by neutron activation of the natural cobalt. Finally, these activated species are redistributed in the cooling circuit and subsequently, deposited on the system surfaces which are exposed to reactor water. This activity transport and the build-up of radiation fields may result in increased occupational doses of radiation for the personnel of the plant. A novel method to decrease the activity incorporation is injection of zinc into the primary coolant. The exact mechanisms by which zinc affects are not known, but one possibility is the competition between zinc and cobalt for the adsorption sites, as discussed by Mäkelä et al. (1999) in a recent literature survey. In addition to the transport of harmful species, the properties of these oxide films formed on the piping surfaces influence the susceptibility to corrosion phenomena taking place on the surfaces. To minimise the risks involved in these harmful processes, a better understanding of the behaviour of the metal oxides in aqueous environments is required.

During the last few years extensive research has been carried out at VTT Manufacturing Technology to increase understanding of the behaviour of oxide films formed on construction materials in nuclear power plant conditions. These studies are published in a series of papers by Bojinov and co-workers (Bojinov et al. 2000a, b, c; Beverskog et al. 2000a, b), who have employed sophisticated electrochemical techniques to study the phenomena taking place mainly in the compact oxide layer and at its interfaces. Although there is still some uncertainty about the composition of the formed oxide films, its is generally believed that a compact layer normally forms at the early stages of oxidation. Further oxidation leads to the formation of a porous oxide layer on top of the compact one. The work started in this project and reported in this and a parallel report (Lehikoinen and Olin 2000) is the first step to extend the research conducted at VTT to include the transport and adsorption phenomena taking place in the outer, porous layer of the oxide film and at the film–coolant interface. Analogous phenomena have been studied at VTT Chemical Technology by means of the surface complexation approach in applications concerning the release of radionuclides from final repositories and the flotation of minerals. In the present project the knowledge of surface complexation acquired at VTT Chemical Technology is applied in a joint effort to understand the adsorption phenomena in the transport of radioactivity in water-cooled nuclear reactors.

The work carried out at VTT focuses on modelling the transport of species through the films as well as the interfacial reactions and adsorption phenomena at the film–solution interface in such a way that the rate-limiting steps for the dissolution and incorporation of the species can be recognised. Our ultimate goal is to present a model for the transport of the species (dissolution and incorporation) through the whole oxide film consisting of different layers with different physical and chemical properties. The results will increase the understanding of the correlations between applied water chemistry and different corrosion and activity incorporation processes. This in turn will facilitate the control of the rates of the dissolution and incorporation of the species, preferably by means of the monitoring facilities existing at the plants and thus, to influence the rates of different types of corrosion and activity incorporation.

Three main tasks for the present subproject can be defined: a literature review on selected aspects of the surface chemistry of iron oxides, model calculations on the adsorption of zinc and cobalt on iron oxide and creating a first version of the transport model in the porous layer. The first two tasks are reported here, while the transport modelling is the subject of a parallel report (Lehikoinen and Olin 2000). As will be discussed below, adsorption of inorganic solutes on oxide surfaces is nowadays most frequently modelled by employing the surface complexation approach. Due to the importance of this approach also for our further studies, we use in this first report a considerable amount of space and effort to present the main concepts and various implementations of the surface complexation models in sufficient detail. The examples deal with iron oxides, but the treatment is more general. Based on the literature studies, we have for the moment chosen one specific iron oxide, ferrihydrite known also as hydrous ferric oxide, as the model sorbent to be used in our adsorption calculations. In these calculations we rely on the thermodynamic data compiled by Dzombak and Morel (1990) and consequently, adopt also their surface complexation model, the generalized two-layer model. The movement of species within the porous oxide film is largely regulated by an interplay of retention (adsorption and redeposition) and transport phenomena. A conceptual model that accounts for these coupled processes is presented in the report by Lehikoinen and Olin (2000). Along with the compilation by Dzombak and Morel (1990), the book by Cornell and Schwertmann (1996) turned out to be invaluable and is highly recommended for everyone interested in iron oxides.

## 1.1 Approach taken in this study

While considering the competitive interaction of various dissolved ions with the oxide film, we assume the first step to be adsorption. Further, we use the surface complexation approach to elucidate the effects that solution conditions have on adsorption. In contrast to the classical adsorption models, surface complexation models represent adsorption in terms of interaction of the adsorbate with the surface OH groups of the adsorbent oxide resulting in the formation of specific surface complexes. Consequently, this approach provides a thermodynamically consistent framework for modelling the distribution of solutes between aqueous solution and oxide surfaces and supplies a quantifiable basis for assessing the identity of those surface species that may act as precursors in further surface-controlled processes. While there is still much work needed in these areas, the potential for prediction of metal ion sorption on a field scale using surface complexation models is evident and a way is available to incorporate a state-of-the-art description of adsorption in transport models.

# 2. Iron oxides

According to Cornell and Schwertmann (1996), there are sixteen different iron oxides, which are listed in Table 1. As is obvious from Table 1, these compounds are in fact oxides, hydroxides or oxide hydroxides, but they are generally collectively referred to as iron oxides. It is also noteworthy that there are five polymorphs of FeOOH and four of $Fe_2O_3$. Goethite, lepidocrocite, ferrihydrite (known also as hydrous ferric oxide), hematite, magnetite and maghemite are common minerals in nature. Akaganéite, schwertmannite and feroxyhyte occur rarely in nature while bernalite has only been found as a sample in a museum and $Fe(OH)_2$ does not exist as a mineral. Wüstite is an important intermediate in the reduction of iron ores, while $\delta$-FeOH, $\beta$-$Fe_2O_3$, $\varepsilon$-$Fe_2O_3$ and high-pressure FeOOH are synthetic laboratory products.

*Table 1. The various iron oxides according to Cornell and Schwertmann (1996, p. 2).*

| Oxide hydroxides and hydroxides | Oxides |
|---|---|
| | |
| Goethite, $\alpha$-FeOOH | Hematite, $\alpha$-$Fe_2O_3$ |
| Lepidpcrocite, $\gamma$-FeOOH | Magnetite, $Fe_3O_4$ |
| Akaganéite, $\beta$-FeOOH | Maghemite, $\gamma$-$Fe_2O_3$ |
| Schwertmannite, $Fe_{16}O_{16}(OH)_y(SO_4)_z \cdot n\ H_2O$ | $\beta$-$Fe_2O_3$ |
| $\delta$-FeOOH | $\varepsilon$-$Fe_2O_3$ |
| Feroxyhyte, $\delta'$-FeOOH | Wüstite, FeO |
| High pressure FeOOH | |
| Ferrihydrite, $Fe_5HO_8 \cdot 4\ H_2O$<br>also known as hydrous ferric oxide, $Fe_2O_3 \cdot n\ H_2O$ (n = 1…3) | |
| Bernalite, $Fe(OH)_3$ | |
| $Fe(OH)_2$ | |

## 2.1 Oxide films

Upon exposure to water, iron corrodes resulting in the release of $Fe^{2+}$ and $Fe^{3+}$ ions into the solution. Parallel to this oxidation, a cathodic reaction takes place. Depending on the conditions, this reaction can be the reduction of dissolved oxygen to produce hydroxyl ions, which react directly with the dissolved iron to produce an oxide precipitate. The iron oxide phases, that will form when iron corrodes, depend on a wide range of chemical, physical and hydrodynamic conditions. As noted by Cornell and Schwertmann (1996, p. 451), all the major iron oxides have been identified in the corrosion products of iron and steel.

Thermodynamic considerations, summarized in Pourbaix diagrams, can be used to indicate the conditions under which different types of corrosion behaviour may be expected. However, there exist conditions under which corrosion would be expected to accelerate, but instead decreases to a negligible value; the passive domain. This passivity is due to the formation of an oxide film that adheres firmly to the metal and prevents its further oxidation by forming a barrier to the transport of reacting species.

Laitinen et al. (1999) have recently accomplished a literature review where they collected and evaluated the present views on the structure and behaviour of the oxide films formed on iron, steels and engineering alloys, with special regard to questions related to coolant systems in nuclear power plants. The nature and properties of these metal oxide films depend strongly on the environment to which the material is exposed. At ambient temperatures (i.e. below about 100 °C) very thin films, characteristically a few nanometers thick, are formed, but at elevated temperatures, ranging from 200 °C to 300 °C, actual in nuclear power plant conditions, noticeable changes in oxide films take place. Above 150 °C, rather thick oxide films are formed, and a more or less pronounced enrichment or depletion of alloy constituents can be found. According to the literature reviewed by Laitinen et al. (1999), the films formed on the surfaces of iron- and nickel-based alloys in high-temperature aqueous environments generally comprise two layers, i.e. they have a duplex structure. The inner layer of a duplex film is normally enriched in chromium and consists of fine-grained oxide because it grows within a confined space. On the other hand, the outer layer consists of loosely packed, larger grains, because it grows without volume constraint.

In this project we focus on the transport phenomena through the outer layer of the oxide film and on the adsorption at the oxide–solution interface. The composition of the outer, deposited, oxide is known to be clearly influenced by the properties of the aqueous environment and under oxidising conditions it is generally assumed to have the hematite structure. Further, we assume that the very outermost layer is more or less hydrated and poorly ordered resembling ferrihydrite. Despite the uncertainty in the exact composition and structure of the passive iron oxide film, it is evident that the hydrated passive film on iron and steels displays the coordinative properties of the Fe(lll) surface hydroxyl groups enabling the application of the surface complexation approach in adsorption modelling.

## 2.2 Ferrihydrite

In this chapter, based on the books by Dzombak and Morel (1990) and Cornell and Schwertmann (1996), we briefly discuss the nature of the iron oxide termed ferrihydrite which has been a classical sorbent for adsorption studies. As ferrihydrite is also known to be a precursor of hematite, we use it as the model for the interface layer between the oxide film and the aqueous coolant. In fact, Dzombak and Morel (1990) distinguish between the natural mineral ferrihydrite and a synthetic product hydrous ferric oxide

(HFO) which has also been termed amorphous iron oxide, amorphous iron hydroxide, amorphous ferric hydroxide and amorphous iron oxyhydroxide. We, however, adopt the terminology of Cornell and Schwertmann (1996) and use the term ferrihydrite for both the natural mineral and for the synthetic precipitate.

Unlike other iron oxides, both synthetic and natural ferrihydrite are poorly ordered. Further, the degree of ordering of various ferrihydrite samples varies and consequently, a range of XRD patterns may be obtained. According to Cornell and Schwertmann (1996), the two extremes of ordering are referred to as 2-line and 6-line ferrihydrite, because the XRD patterns range from two to six reflections as structural order increases. Neither the exact structure nor the formula of ferrihydrites have been fully established. According to Cornell and Schwertmann (1996), the structure resembles that of hematite and the composition is given by the formula $Fe_5HO_8 \cdot 4\ H_2O$. Dzombak and Morel (1990), however, denote the chemical composition of ferrihydrite by the general formula $Fe_2O_3\ n\ H_2O$ (n=1…3) and note that due to the high water content and disordered bulk structure, ferrihydrite resembles a swollen gel more than a homogeneous solid phase.

Ferrihydrite forms in aqueous solutions by direct precipitation from soluble Fe(lll) species under conditions where the more stable phases goethite, akaganéite and lepidocrocite do not form. The conditions for ferrihydrite formation, along with instructions for laboratory synthesis, are discussed in detail by Cornell and Schwertmann (1996), but generally rapid hydrolysis of $Fe^{3+}$ solutions or oxidation of $Fe^{2+}$ solutions followed by rapid hydrolysis results in the formation of ferrihydrite. However, which type of ferrihydrite (e.g. 6-line or 2-line) or even which oxide forms, is governed by solution conditions, such as pH, temperature, concentrations of dissolved ions and possibly, the oxidation rate of $Fe^{2+}$ ions. With extended aging in aqueous solutions ferrihydrite gradually transforms to crystalline iron oxide, usually hematite or goethite, the ratio between them depending mainly on the kinetics of the interconversion reactions. In nature, the reddish–brown ferrihydrite is widespread in surface environments. Ferrihydrite formation is also a common initial phase in the genesis of other iron oxides, but due to its metastable nature, it can be expected as a soil constituent mainly in relatively young soils or in those where its transformation to more stable oxides is inhibited or retarded. For example, a high rate of Fe(ll) oxidation and the presence of organic compounds such as humics promote ferrihydrite formation because these factors impede the formation of crystalline iron oxides.

# 3. Modelling surface complexation on iron oxides

Nowadays it is generally accepted that in humid environments iron oxide surfaces are covered with surface hydroxyl groups, ≡Fe–OH. The origin of these surface hydroxyl groups is schematically depicted in Figure 1. The surface of a dry iron oxide is characterized by the presence of low-coordinated ferric ions (A) giving rise to Lewis acidity. Initially, the addition of water leads to coordination of $H_2O$ molecules to these coordinatively undersaturated metallic centers (B). Dissociative chemisorption (C) under formation of hydroxyl groups seems, however, to be energetically favoured resulting in the formation of surface OH groups, ≡Fe–OH.

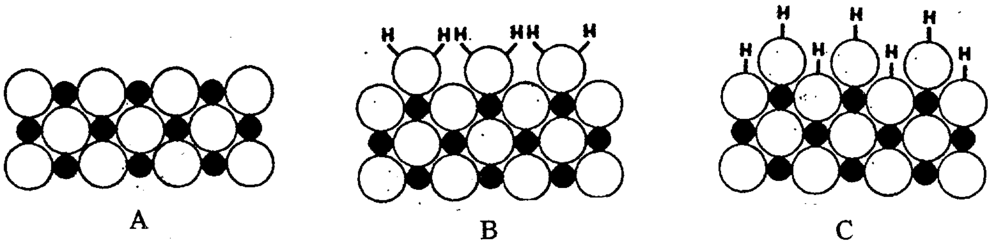

*Figure 1. Cross section of the surface layer of a metal oxide: (●) metal ions, (❍) oxide ions. A) Surface ions show low coordination and exhibit Lewis acidity. B) In the presence of water, surface metal ions may coordinate $H_2O$ molecules. C) Dissociative chemisorption leads to a hydroxylated surface. From Schindler (1981).*

The presence of two lone electron pairs and a dissociable hydrogen ion indicates that these groups are ampholytes being able to react as follows:

$$\equiv\text{Fe–OH} + H^+ = \equiv\text{Fe–OH}_2^+ \qquad (1)$$

$$\equiv\text{Fe–OH} = \equiv\text{Fe–O}^- + H^+ \qquad (2)$$

In addition to the adsorption and desorption of protons, adsorption of metal ions and anions is well established and explained by Lewis-base behaviour of deprotonated surface hydroxyls and by ligand exchange. The adsorption of metal ions will be discussed in detail below, but generally cation adsorption is accompanied with a release of protons as illustrated by equation (3). Anion adsorption is generally considered as involving replacement of the surface hydroxyl groups by the adsorbing anion (i.e. ligand), L, as illustrated by equation (4).

$$\equiv\text{FeOH} + \text{Me}^{z+} = \equiv\text{FeOMe}^{(z-1)} + H^+ \qquad (3)$$

$$\equiv\text{FeOH} + L^- = \equiv\text{FeL} + OH^- \qquad (4)$$

In this chapter the fundamental principles of surface complexation modelling are demonstrated using the most elementary system, the hydrolysis on the iron oxide surface described by reactions (1) and (2) as an example. The surface hydrolysis can be defined as adsorption of $H^+$ and $OH^-$ ions, the former being described by equation (1), whereas the uptake of hydroxyl ions can be presented as the deprotonation reaction (2) followed by $H^+ + OH^- = H_2O$ (Schindler and Gamsjäger 1972; Westall 1986). Although the main interest in this project is to understand the adsorption of cobalt and zinc ions on iron oxides, not the adsorption of $H^+$ and $OH^-$ ions, we have, for two reasons, chosen the most elementary system to illustrate the surface complexation approach. Firstly, the chemistry of this system is as uncomplicated as it can be, and it also comprises a subset in any study dealing with adsorption of aqueous species on iron oxide surfaces. Secondly, understanding the principles and mathematics of the modelling of this simple system is, in any event, a prerequisite for the understanding of more complicated systems.

The two papers by Schindler and co-workers (1968, 1972) on the constant capacitance model (CCM) and a paper by Stumm et al. (1970) on the diffuse layer model (DLM) introduced the surface complexation approach in its modern form, although the development was an evolutionary process involving contributions from several research groups. Further conceptual milestones in the development of surface complexation modelling were the introduction of the triple layer model by Yates et al. (1974) and its modification by Hayes and Leckie (1987). The diffuse layer model was further modified by Dzombak and Morel (1990) who also accomplished the imposing task of producing a coherent and consistent thermodynamic interpretation of a vast number of sorption reactions on hydrous ferric oxide, which forms the basis of the model calculations done in this study (cf. Chapter 4.5). In addition to the above mentioned seminal papers, the discussion in the following chapters is mainly based on the papers by Westall (Westall 1980, 1982, 1986, 1987; Westall and Hohl 1980), Fornasiero and co-workers (Fornasiero et al. 1992; Wood et al. 1990) and on several reviews on surface complexation modelling (Schindler 1981; Schindler and Stumm 1987; Stumm 1992; Sposito 1984; Goldberg 1992; Hayes and Katz 1996; Jenne 1998). The book of Sposito (1984) is especially recommended for those who are interested in a thermodynamically rigorous treatment of the subject, while the mathematical formulation is clearly presented by Westall (Westall 1980; Westall and Hohl 1980).

## 3.1 Formulation of the problem

The aim of surface complexation modelling is to describe the experimental sorption data over the widest possible range of experimental conditions by means of reactions taking place at the oxide–water interface and in the solution. For this purpose the reactions have first to be defined and then, quantified by means of equilibrium constants. When these data are available, the speciation in the system can be calculated and presented as a function of parameters such as pH or $-\log Me^{n+}$, where $Me^{n+}$ indicates the ion whose adsorption is studied. As discussed below, there exist several different surface complexation models, but all of them are expressed with similar material balance and mass law equations, which in the present case are written as follows:

$$[\equiv\text{Fe–OH}]_{\text{tot}} = T_{\equiv\text{Fe–OH}} = [\equiv\text{Fe–OH}] + [\equiv\text{Fe–O}^-] + [\equiv\text{Fe–OH}_2^+] \qquad (5)$$

$$[\text{H}^+]_{\text{tot}} = T_{\text{H}} = [\text{H}^+] - [\text{OH}^-] + [\equiv\text{Fe–OH}_2^+] - [\equiv\text{Fe–O}^-] \qquad (6)$$

$$K_+ = \frac{[\equiv\text{Fe}-\text{OH}_2^{\;+}]}{[\equiv\text{Fe}-\text{OH}][\text{H}^+]} \qquad (7)$$

$$K_- = \frac{[\equiv\text{Fe}-\text{O}^-][\text{H}^+]}{[\equiv\text{Fe}-\text{OH}]} \qquad (8)$$

The subscript tot in the material balance equations is used to indicate the total, i.e. analytical, concentration of surface hydroxyl groups or strong acid/strong base in the system.

Because of using concentrations instead of activities in the mass balance equations, the “constants” $K_+$ and $K_-$ are apparent constants, valid for a given electrolyte medium. In fact, even for a given electrolyte medium they are not constants due to the variable electrostatic energy of interaction caused by the variable charge on the surface which originates from the sorption reactions themselves. Although it is impossible to separate experimentally the chemical and electrical contributions to the total interaction energy, it is useful to separate them theoretically in order to obtain a specific (i.e. chemical) interaction term that does not vary with surface charge. A variable electrostatic interaction term may then be added, resulting in a model that accounts for observed variations in apparent equilibrium constants:

$$\Delta G = \Delta G_{\text{chem}} + \Delta G_{\text{elect}} \qquad (9)$$

Inserting the general relationship $\Delta G = -RT \ln K$ into this equation (9), defining the zero level of the potential in the bulk of the solution and indicating the potential of the mean plane of adsorption of protons with $\psi_0$ (less rigorously $\psi_0$ can be called the surface potential) we obtain for reaction (1)

$$\Delta G = -RT \ln K_+ = \Delta G_{\text{chem}} + \Delta G_{\text{elect}} = -RT \ln K_2 + zF\psi_0 \qquad (10)$$

The last term in this equation indicates the electrostatic work needed to transfer one mole of ions ($F$ is the Faraday constant 96 485 C/mol) having the charge number $z$ from the solution ($\psi = 0$) to the surface ($\psi_0$). The equilibrium constant[*] $K_2$ corresponds to the chemical part of the adsorption energy and is called an intrinsic equilibrium constant. Traditionally, its value has been found by extrapolation of experimental data to zero surface charge conditions where the electrostatic energy term, $zF\psi_0$, vanishes. From this equation (10) it is evident that in the case of reaction (1) ($z = 1$)

---

[*] The somewhat strange subscript 2 is chosen for reasons that will become apparent later.

$$K_+ = K_2 \exp(-F\psi_o/RT) \quad (11)$$

which can be combined with equation (7) to give

$$[\equiv\text{Fe–OH}_2^+] = K_2 \exp(-F\psi_o/RT)\, [\equiv\text{Fe–OH}]\, [\text{H}^+] \quad (12)$$

In a similar way, using equation (2) as a starting point we obtain

$$[\equiv\text{Fe–O}^-] = K_3 \exp(+F\psi_o/RT)\, [\equiv\text{Fe–OH}]\, [\text{H}^+]^{-1} \quad (13)$$

where the positive sign of the exponent is due to the fact that we are considering the transfer of the proton from the surface with potential $\psi_o$ into the solution where $\psi = 0$, and not vice versa.

When modelling the system, in addition to reactions (1) and (2), we have to consider the autoprotolysis of water taking place in any aqueous system. For the reaction

$$\text{H}_2\text{O} = \text{H}^+ + \text{OH}^- \quad (14)$$

we can write

$$[\text{H}^+][\text{OH}^-] = K_1 \quad (15)$$

$$[\text{OH}^-] = \frac{K_1}{[\text{H}^+]} \quad (16)$$

Taking logarithms of both sides of equations (16), (12) and (13), we obtain

$$\log[\text{OH}^-] = \log K_1 - \log[\text{H}^+]^* \quad (17)$$

$$\log[\equiv\text{Fe–O}^-] = \log K_3 - \log e^{-F\psi o/RT} + \log[\equiv\text{Fe–OH}] - \log[\text{H}^+] \quad (18)$$

$$\log[\equiv\text{Fe–OH}_2^+] = \log K_2 + \log e^{-F\psi o/RT} + \log[\equiv\text{Fe–OH}] + \log[\text{H}^+] \quad (19)$$

Further, we can write the following trivial identities:

$$\log[\text{H}^+] = \log 1 + \log[\text{H}^+] \quad (20)$$

$$\log[\equiv\text{Fe–OH}] = \log 1 + \log[\equiv\text{Fe–OH}] \quad (21)$$

$$\log e^{-F\psi o/RT} = \log 1 + \log e^{-F\psi o/RT} \quad (22)$$

---

[*] $-\log[\text{H}^+]$ should be understood as the shorthand notation for $-\log_{10}([\text{H}^+]/\text{M})$

The important point about equations (17–22) is that the concentrations of all the chemical species in the system depend only on equilibrium constants, the concentrations of $H^+$ and ≡Fe–OH and the term $e^{-F\psi o/RT}$, which results from the electrostatic effects distinctive for reactions taking place on the surface. The last term would be omitted if only solution reactions were to be considered. In that case, the concentrations of all the chemical entities of the system, the species, could be expressed by equations containing only constants and the concentrations of a smaller number of chemical entities, the components. Although, this definition of components differs from that given in most thermodynamics textbooks, it is widely used in solution chemistry and will be employed accordingly in this text. It should be noted that the set of components is defined in a way that every species can be written as the product of a reaction involving only the components and no component can be written as the product of a reaction involving only the other components. The set of components is certainly not unique, but once it has been defined, the representation of the species in terms of this set of components is unique. By studying equations (17–22), it is obvious that the electrostatic correction factor $e^{-F\psi o/RT}$ can be formally treated as a chemical component, which has been first shown by Westall (1980). Consequently, surface complexation models easily fit in the mathematical framework of chemical equilibrium models. After rearranging, the logarithmic mass law equations (17–22) are conveniently expressed in a matrix form

$$\begin{vmatrix} \log[\mathrm{H}^+] \\ \log[\mathrm{OH}^-] \\ \log[\mathrm{Fe-OH}_2^+] \\ \log[\mathrm{Fe-OH}] \\ \log[\mathrm{Fe-O}^-] \end{vmatrix} = \begin{vmatrix} \log 1 \\ \log K_1 \\ \log K_2 \\ \log 1 \\ \log K_3 \end{vmatrix} + \begin{vmatrix} 0 & 0 & 1 \\ 0 & 0 & -1 \\ 1 & 1 & 1 \\ 1 & 0 & 0 \\ 1 & -1 & -1 \end{vmatrix} \bullet \begin{vmatrix} \log[\mathrm{Fe-OH}] \\ \log \mathrm{e}^{-F\psi o/RT} \\ \log[\mathrm{H}^+] \end{vmatrix} \qquad (23)$$

written in a shorter way as

$$\boldsymbol{C} = \boldsymbol{K} + \boldsymbol{A}\,\boldsymbol{X} \qquad (24)$$

where the meaning of the symbols $\boldsymbol{C}$, $\boldsymbol{K}$, $\boldsymbol{A}$, and $\boldsymbol{X}$ is obvious. Matrix $\boldsymbol{A}$ is called the stoichiometric matrix and it consists of stoichiometric coefficients of the components in the species. The absence of water in the above equations is explained by the fact that its concentration is considered to be constant, 55.5 M.

In addition to the material balance equations (5) and (6), a further balance equation for the surface charge can be written as

$$(sa\sigma)/F = T_\sigma = [\equiv\mathrm{Fe–OH}_2^+] – [\equiv\mathrm{Fe–O}^-] \qquad (25)$$

implying one of the fundamental assumptions of all the surface complexation models, i.e., the surface charge results from the sorption reactions themselves. The first term in this equation is the molar amount of the surface charge calculated from the concentration of the suspended solid, $a$ [g/dm$^{-3}$], its specific surface area, $s$ [m$^2$/g], and the specific surface charge, $\sigma$ [C/m$^2$]. It is convenient to express even the balance equations in the following matrix form:

$$\begin{vmatrix} T_{\equiv\mathrm{Fe-OH}} \\ T_{\sigma} \\ T_{\mathrm{H}} \end{vmatrix} = \begin{vmatrix} [\equiv\mathrm{Fe-OH_2^+}]+[\equiv\mathrm{Fe-OH}]+[\equiv\mathrm{Fe-O^-}] \\ [\equiv\mathrm{Fe-OH_2^+}]-[\equiv\mathrm{Fe-O^-}] \\ [\mathrm{H^+}]-[\mathrm{OH^-}]+[\equiv\mathrm{Fe-OH_2^+}]-[\equiv\mathrm{Fe-O^-}] \end{vmatrix}$$

$$= \begin{vmatrix} 0 & 0 & 1 & 1 & 1 \\ 0 & 0 & 1 & 0 & -1 \\ 1 & -1 & 1 & 0 & -1 \end{vmatrix} \bullet \begin{vmatrix} [\mathrm{H^+}] \\ [\mathrm{OH^-}] \\ [\equiv\mathrm{Fe-OH_2^+}] \\ [\equiv\mathrm{Fe-OH}] \\ [\equiv\mathrm{Fe-O^-}] \end{vmatrix} \qquad (26)$$

written in a shorter way as

$$\boldsymbol{T} = \boldsymbol{A}^{\mathrm{t}}\ \boldsymbol{C} \qquad (27)$$

where it has been noticed that the matrix, $\boldsymbol{A}^{\mathrm{t}}$, is the transpose of the stoichiometry matrix, $\boldsymbol{A}$, as defined in equations (23) and (24).

As shown above, the mass law equations can be formulated by means of three components ≡Fe–OH, $\mathrm{H^+}$, and $\mathrm{e}^{-F\psi_o/RT}$. The material balance equations for the components ≡Fe–OH and $\mathrm{H^+}$ are obvious, but to be able to include the electrostatic component, $\mathrm{e}^{-F\psi_o/RT}$, in the balance equations, some functional relationship $\sigma = \sigma(\psi_o)$ must be inserted into equation (25).

## 3.2 Relationship between surface charge and potential, various surface complexation models

At this point the various surface complexation models differ from each other, and several functional relationships based on different descriptions of the solid–solution interface layer, the electrical double layer, have been proposed. Helmholtz, who was the first one to think consequentially about charge separation at solid–solution interfaces, proposed that the counter charge in solution also resides on the surface. Thus, there would be two sheets of charge, having opposite polarity, separated by a distance of molecular order. Such a structure is equivalent to a parallel-plate capacitor, which has the following relation between the stored charge density, $\sigma_o$ [C/m$^2$ ], and the potential difference, $\psi_o - \psi_{\mathrm{solution}} = \psi_o - 0 = \psi_o$ [V], between the plates

$$\sigma_o = (\varepsilon\varepsilon_o/d)\,\psi_o \tag{28}$$

where $\varepsilon$ is the dimensionless dielectric constant of the medium, $\varepsilon_o$ is the permittivity of free space ($8.85419 \cdot 10^{-12}$ $C^2$ $N^{-1}$ $m^{-2}$), and $d$ [m] is the interplate spacing. This equation implies a constant value for the specific differential double layer capacitance $C_{dH}$ [$F/m^2 = C/(V\,m^2)$],

$$C_{dH} = \frac{d\sigma_o}{d\psi_o} = \frac{\varepsilon\varepsilon_o}{d} \tag{29}$$

and as a direct consequence of the Poisson equation, a linear potential profile through this layer.

In most electrochemical systems this is, however, not the case, but experience has shown that the capacitance varies with potential and solution composition. It turns out that the assumption of the countercharge in solution residing on the surface is in the general case too simple. Due to thermal motion some significant thickness of solution is needed in order to accumulate enough charge ($\sigma_d$) to counterbalance the charge on the solid surface ($\sigma_o$), that is, a diffuse layer of charge is consequently obtained in the solution. Having described this diffuse layer by a statistical mechanical approach Gouy and Chapman independently were able to derive expressions for the potential profile in the solution side of the interface. When this expression is combined with Gauss' law in the simplest case of a solution of a single, valence-symmetrical ($|z_+| = |z_-| = z$) electrolyte having concentration $c$, a relationship between $\sigma_o$, $\sigma_d$ and $\psi_o$

$$\sigma_o = -\sigma_d = (8RT\varepsilon\varepsilon_o c)^{1/2} \sinh (zF\psi_o/2RT) \tag{30}$$

can be derived implying the following expression for the differential capacitance

$$C_{dGC} = (zF/RT)\,(2RT\varepsilon\varepsilon_o c)^{1/2} \cosh (zF\psi_o/2RT) \tag{31}$$

According to equation (31), there is an unlimited rise in the differential capacitance with $\psi_o$, which, of course, is not realistic. This failure is mainly due to the assumption that the ions are point charges which, consequently, can approach the surface arbitrarily closely.

The Gouy–Chapman model has been further developed by Stern who considered the finite size of the ions prohibiting them from approaching the surface any closer than the ionic radius. Consequently, a plane of closest approach for the centers of the ions can be defined at some distance $x_2$ and is termed the outer Helmholtz plane (OHP). The solution layer between the outer Helmholtz plane and the solid surface is called the Helmholtz or the compact layer, and the layer between the outer Helmholtz plane and the bulk of the solution is called the Gouy or the diffuse layer and can be treated electrostatically as above. If we exclude specific adsorption, the charge density in the compact layer is zero which, in turn, implies, as a direct consequence of the Poisson equation, that the potential profile in this layer is linear. Combining this result with the Gouy–Chapman model for the diffuse layer, a potential profile through the electrochemical double layer can be obtained and is depicted in Figure 2A.

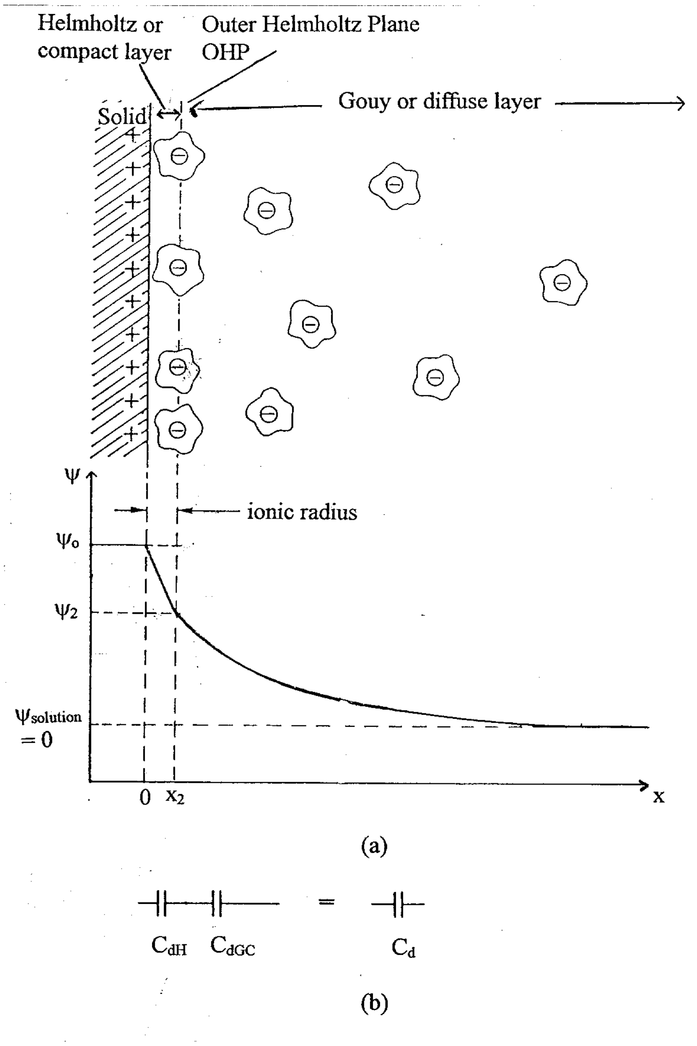

*Figure 2. (A) Structure of the electrical double layer in the absence of specific adsorption and electric potential distribution at solid–solution interface according to the Gouy–Chapman–Stern theory. (B) Description of the composite double layer capacitance as a series network of Helmholtz layer and diffuse layer capacitances. Modified from Hamann and Vielstich (1985) and Bard and Faulkner (1980).*

Using the potential profile obtained, it is possible to derive the charge–potential relationship and an expression for the differential capacitance of the solid–solution interface:

$$C_\mathrm{d} = \frac{(2\varepsilon\varepsilon_o z^2 F^2 c / RT)^{1/2} \cosh(zF\psi_2 / 2RT)}{1 + (x_2 / \varepsilon\varepsilon_o)(2\varepsilon\varepsilon_o z^2 F^2 c / RT)^{1/2} \cosh(zF\psi_2 / 2RT)} \qquad (32)$$

which is more simply expressed as the inverse of capacitance:

$$\frac{1}{C_\mathrm{d}} = \frac{x_2}{\varepsilon\varepsilon_o} + \frac{1}{(2\varepsilon\varepsilon_o z^2 F^2 c / RT)^{1/2} \cosh(zF\psi_2 / 2RT)} \qquad (33)$$

where $\psi_2$ indicates the potential at the outer Helmholtz plane, at the distance $x_2$ from the surface. This expression says that the capacitance is made up of two components that can be separated in the reciprocal, in the same way as one would find for two capacitors in series. Further, we can identify the terms in equation (33) as the reciprocals of the Helmholtz capacitance, $C_\mathrm{dH}$ (29), and the diffuse layer capacitance, $\mathrm{C}_\mathrm{dGC}$ (31):

$$\frac{1}{C_\mathrm{d}} = \frac{1}{C_\mathrm{dH}} + \frac{1}{C_\mathrm{dGC}} \qquad (34)$$

It is obvious that the constant term, $C_\mathrm{dH}$, corresponds to the capacitance of the charges held at the outer Helmholz plane, and can be called compact layer capacitance, whereas, $C_\mathrm{dGC}$ is the capacitance of the truly diffuse layer and depends on both potential and solution composition. In addition to equation (34), this relationship between the three capacitances is also depicted in Figure 2B. The composite capacitance is governed by the smaller of the two components and in certain conditions it can be approximated as being equal to one of them.

In this chapter, following the standard electrochemistry texts (e.g. Bard and Faulkner 1980, pp. 8–10, 500–511; Hamann and Vielstich 1985, pp. 149–160), an attempt has been made to show briefly that using electrostatic and statistical mechanical theories, it is possible to obtain various theoretical relationships between surface charge and potential. Originally, these models were developed for metal–solution interfaces in the case of electrodes, but they are generally applied also to the oxide–solution interfaces. In the above discussion we were not interested in the origin of the charge on the solid phase, but only considered the electrostatic effects creating the balancing excess of the counter ions on the solution side of the interface. Aside from the magnitude of the charges on the ions, and in the Stern modification of their radii, we ignored their chemical identities. Traditionally in electrochemistry, these ions which are kept in the interfacial region only by long-range coulombic interactions are called non-specifically adsorbed ions. Ions become specifically adsorbed when short-range interactions between them and the surface become important. These ions penetrate into the inner layer (Helmholtz layer, compact layer) and may (but not necessarily) come in a direct contact with the solid surface (IUPAC 1983). We are aware of the fact that in surface complexation modelling this nomenclature is not always used and acknowledge that there are good reasons for this. The ions accumulated in the diffuse layer, which we call non-specifically adsorbed ions, are not adsorbed at all in the sense that there is no close-range interaction between them and the surface. However, our terminology is in accordance with the IUPAC definition of adsorption as the enrichment of of one or more components in an interfacial layer (IUPAC 1972).

In the case of oxides the charge on the surfaces may originate from the reactions of the ionizable surface functional groups (eq. 1 and 2) or from processes in which solutes become coordinatively bound to the the surface (eq. 3). In the next chapters we show how the models for electrified interfaces have been used by coordination chemists in their attempts to understand and predict sorption phenomena at oxide surfaces by the means of surface complexation. We will shortly discuss three of the most common surface complexation models, which have inherited the names: the constant capacitance model, the diffuse layer model and the triple layer model. A general perception is that these models differ significantly, but especially the two first mentioned are closely related, and they can be considered limiting cases of the more elaborate triple layer model. The models differ principally in the number of considered separate layers at the oxide–solution interface and, consequently, in the location of various adsorbing species. As a consequence, the electrostatic equations which are used to relate surface potential to surface charge, i.e., the way in which free energy of adsorption is divided into its chemical and electrostatic components, are different for each model. In addition to showing the electrostatic aspects of these models, we use the simplest of them, the constant capacitance model, to illustrate how model parameters can be extracted from titration data.

### 3.2.1 Constant capacitance model

The constant capacitance model was introduced to surface complexation studies by Schindler and Gamsjäger in 1972. In this simple two-layer model, illustrated in Figure 3, all the specifically adsorbed ions are considered to be part of the solid surface experiencing the potential $\psi_o$. The resulting electric charge of the surface is balanced by an adjacent planar layer of counter-ions in solution, implying a constant capacitance and a linear potential profile between the surface and the solution. By studying equations (31) and (34), it can be shown that in high electrolyte concentrations, or even at high potential differences in dilute media, $C_{dGC}$ becomes so large that it no longer contributes to $C_d$, which can be approximated equal to the constant component $C_{dH}$ resulting in relationship (35) between the surface charge and the surface potential

$$\sigma_o = C_d \psi_o \qquad (35)$$

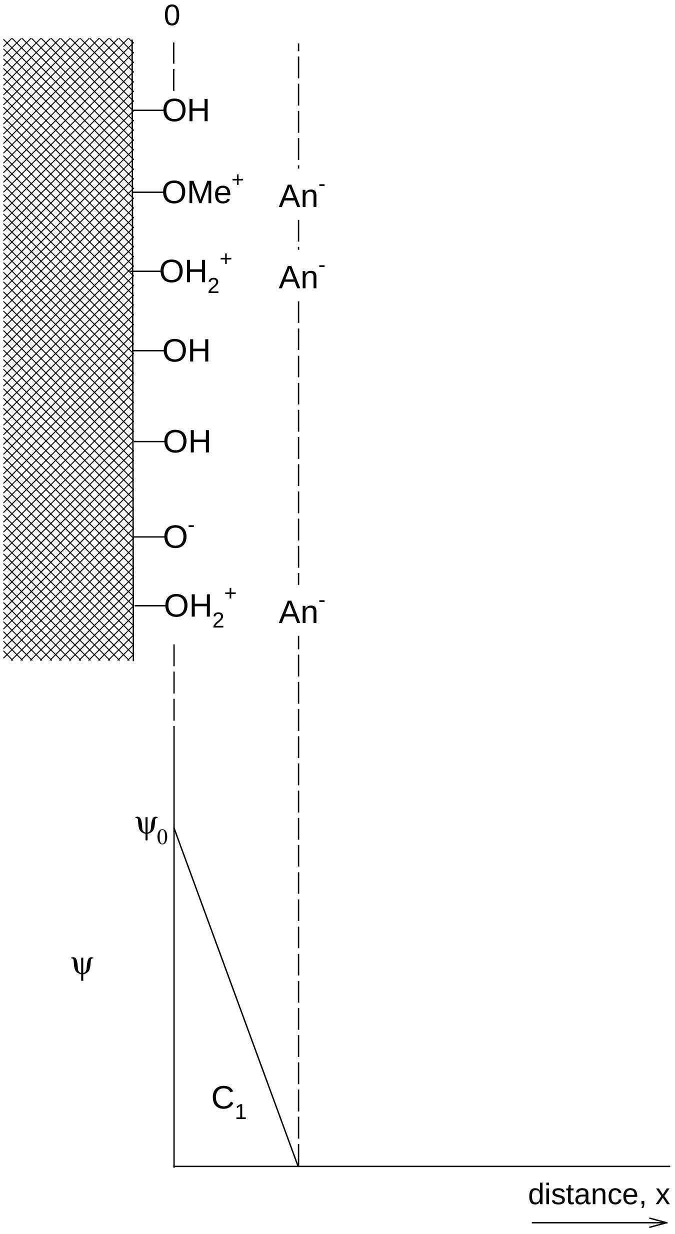

*Figure 3. Potential profile through and location of ions within the electrical double layer according to the constant capacitance model.*

Qualitatively the situation can be interpreted in a way that at high potential differences or with more concentrated electrolytes, the charge in solution becomes more tightly compressed against the outer Helmholtz plane and consequently, the whole system begins to resemble the Helmholtz model. Although in theory, this approximation is valid only in high potential, high ionic strength systems, the model has been succesfully applied also far out of this domain, e.g., at 0.001 M ionic strength (Westall and Hohl 1980).

To give a practical example, we will below use the constant capacitance model and the acid–base reactions (1) and (2) to illustrate the principles for extracting the values of the intrinsic acidity constants from experimental data. At this point we also revert to the common notation of surface complexation modelling considering the acid–base reactions as deprotonations and using $K_{a1}$ and $K_{a2}$ to denote their acidity constants as follows:

$$\equiv\text{Fe–OH}_2^+ = \equiv\text{Fe–OH} + \text{H}^+ \qquad K_{a1} \tag{36}$$

$$\equiv\text{Fe–OH} = \equiv\text{Fe–O}^- + \text{H}^+ \qquad K_{a2} \tag{37}$$

$$K_{a1} = \frac{[\equiv \text{Fe}-\text{OH}][\text{H}^+]}{[\equiv \text{Fe}-\text{OH}_2{}^+]} = K_{a1}^{\text{int}} \exp(F\psi_o / RT) \tag{38}$$

$$K_{a2} = \frac{[\equiv \text{Fe}-\text{O}^-][\text{H}^+]}{[\equiv \text{Fe}-\text{OH}]} = K_{a2}^{\text{int}} \exp(F\psi_o / RT) \tag{39}$$

Reaction (36) is the reverse of reaction (1) which was written as a reaction producing the species $\equiv$Fe–OH$_2^+$ from the components $\equiv$Fe–OH and H$^+$ to ensure the simple form of equation (23). The example below is presented mainly for instructional purposes as usually the parametrs are extracted by a general data fitting procedure utilizing the matrix formulation discussed above. In a more complicated system or in cases where the simplifying assumptions are not acceptable, such a calculation by hand is not even possible.

Inserting the constant capacitance model (35) into the relationship between apparent and intrinsic equilibrium constants (38), we obtain

$$K_{a1} = K_{a1}^{\text{int}} \exp(F\psi_o/RT) = K_{a1}^{\text{int}} \exp(F\sigma_o/C_{d+}RT) \tag{40}$$

which is conveniently expressed in a logarithmic form

$$\text{p}K_{a1} = \text{p}K_{a1}^{\text{int}} - \sigma_o\,(F/C_{d+}\,RT \ln 10) \tag{41}$$

In a similar way we obtain

$$\text{p}K_{a2} = \text{p}K_{a2}^{\text{int}} - \sigma_o\,(F/C_{d-}\,RT \ln 10) \tag{42}$$

where $C_{d+}$ is the specific capacitance for the positively charged surface and $C_{d-}$ is the specific capacitance for the negatively charged surface[*].

The quotients $K_{a1}$ and $K_{a2}$ are experimentally accessible quantities, and by making a simplifying assumption, their values are easily calculated even by hand from acid–base titration data consisting of ($V_{acid}$, pH) and ($V_{base}$, pH) data pairs. Assuming that on the acidic branch of the titration curve the concentration of the $\equiv$Fe–O$^-$ species is negligible and on the basic branch the concentration of the $\equiv$Fe–OH$_2^+$ species is negligible, it is possible to calculate also the surface charge, $Q$ [mol/g], from the titration data. However, a prerequisite for this is that the total amount of reactive surface sites is determined either by a surface titration experiment or by independent means such as tritium exchange or consideration of surface area and crystal structure. By plotting the experimentally available apparent equilibrium constants (p$K_{a1}$ and p$K_{a2}$) against the surface charge, a linear relationship is, indeed, frequently observed making it possible to determine the values of the intrinsic equilibrium constants (p$K_{a1}^{int}$ and p$K_{a2}^{int}$) and the specific capacitances from the intercepts and the slopes of the plots as demonstrated in Figure 4. This figure is taken from the text book by Stumm where an illustrative and detailed example of the above procedure in the case of goethite (α-FeOOH) is given (Stumm 1992, pp. 16–19, 74). The independent variable, $Q$, in Figure 4, is the amount of charged species on the surface divided by the mass of the solid phase and is customarily related to the surface charge, $\sigma_o$ [C/m$^2$ ], by the equation:

$$\sigma_o = QF/s \qquad (43)$$

In this equation $s$ [m$^2$/g] stands for the specific surface area. Due to the assumption that $\equiv$Fe–OH$_2^+$ and $\equiv$Fe–O$^-$ do not coexist, values of p$K_{a1}$ are calculated only when $Q > 0$ and values of p$K_{a2}$ only when $Q < 0$.

---

[*] It is a generally recognized weakness of the constant capacitance model that two different capacitance values, $C_{d+}$ and $C_{d-}$, are usually obtained from the extrapolation method described below (Sposito 1984 p. 174, Goldberg 1992).

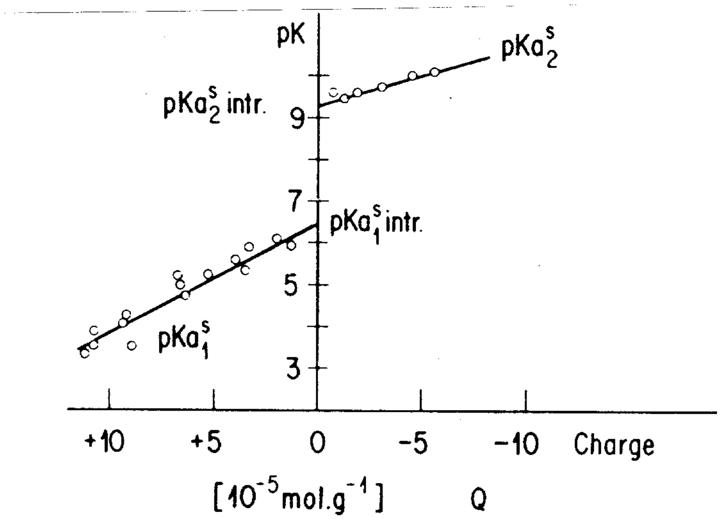

*Figure 4. Conditional equilibrium constants for deprotonation reactions* $\equiv FeOH_2^+ = FeOH + H^+$ *(*$K_{a1}^s$*) and* $\equiv FeOH = FeO^- + H^+$ *(*$K_{a2}^s$*) as a function of charge. Extrapolation to zero charge gives intrinsic constants. From Stumm (1992, p. 17).*

### 3.2.2 Diffuse layer model

The diffuse layer model (DLM) was introduced to surface complexation studies by Stumm and co-workers (Stumm et al. 1970; Huang and Stumm 1973) and has been modified (and renamed as the generalized two-layer model) by Dzombak and Morel (1990) to incorporate strong and weak coordination sites. Similar to the constant capacitance model, the diffuse layer model, as illustrated in Figure 5, is a simple two-layer model in which all the specifically adsorbed ions are considered to be part of the solid surface (one layer). Its electrostatic charge is balanced by an adjacent diffuse layer of counterions in solution (the other layer). A Gouy–Chapman distribution of ions is assumed for the solution side of the interface, but the fixed number of surface sites implicit in every surface complexation model is not a part of the original Gouy–Chapman theory. This implicit limitation constrains the near-surface ion densities to reasonable values representing a modification of the Gouy–Chapman theory similar to that of Stern who took explicitly into account the finite size of the ions. As in the constant capacitance model, all specifically adsorbed ions are assumed to contribute to the charge $\sigma_0$ and experience the potential $\psi_0$. However, in contrast to the constant capacitance model, there is no adjustable capacitance parameter as the capacitance of the interfacial region is taken to be equal to the diffuse layer capacitance for which the theoretical expression (31) is used.

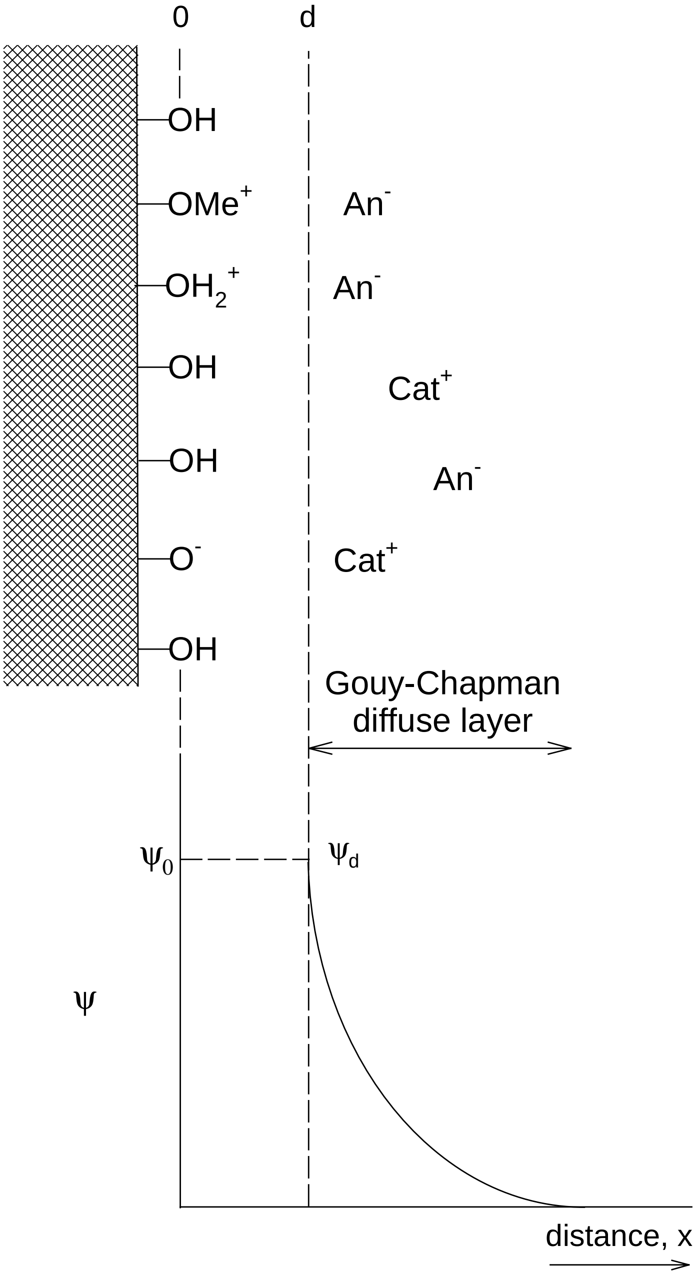

*Figure 5. Potential profile through and location of ions within the electrical double layer according to the diffuse layer model.*

While employing the diffuse layer model to a vast number of published data on cation sorption on ferrihydrite, Dzombak and Morel (1990) noticed that two site types were required to model cation (other than $H^+$) adsorption. Metal ion adsorption is considered to occur on a small set of high affinity (strong) sites and a large set of low-affinity (weak) sites, but usually only one kind of surface complex stoichiometry, $\equiv$FeO–Me$^+$ corresponding to reaction (3), is needed for both site types. Based on crystallographic considerations on various iron oxides (Cornell and Schwertmann 1996, pp. 207–213), the assumption that there are at least two types of surface hydroxyl groups is very reasonable and made also by other researchers (Hayes and Katz 1996).

According to our opinion, the main merit of Dzombak´s and Morel´s (1990) work is, however, not the modification of the diffuse layer model, but the critical compilation of coherent sorption constants. They critically reviewed the sorption literature on ferrihydrite, fitted the relevant inorganic sorption data to the generalized two-layer model and in a systematic way extracted a set of self consistent surface complexation constants. Such a data base is a necessary prerequisite to make sorption calculations a routine tool for a practising chemist.

### 3.2.3 Triple layer model

The triple layer model is a type of extended Gouy–Chapman–Stern model (cf. Figure 2) with the compact double layer split into two parts as illustrated in Figure 6. This enables to consider the specifically adsorbed ions either as inner-sphere complexes or as outer-sphere complexes, where the terminology from coordination chemistry is adopted (Morel and Hering 1993, p. 322; Stumm and Morgan 1981, p. 346; Stumm 1995). Surface complexes formed at the $o$-plane are considered model analogs of inner-sphere complexes whereas, those formed at the $\beta$-plane are considered outer-sphere analogs. Analogously to the complexation in solution, an inner-sphere surface complex contains no water molecule between the surface site (i.e. ligand) and the adsorbed cation (Stumm and Morgan 1981, p. 346), while in an outer-sphere surface complex the adsorbed cation retains its primary hydration shell in a similar way as in the formation of ion pairs (i.e. outer-sphere complexes) in solution (Morel and Hering 1993, p. 322).

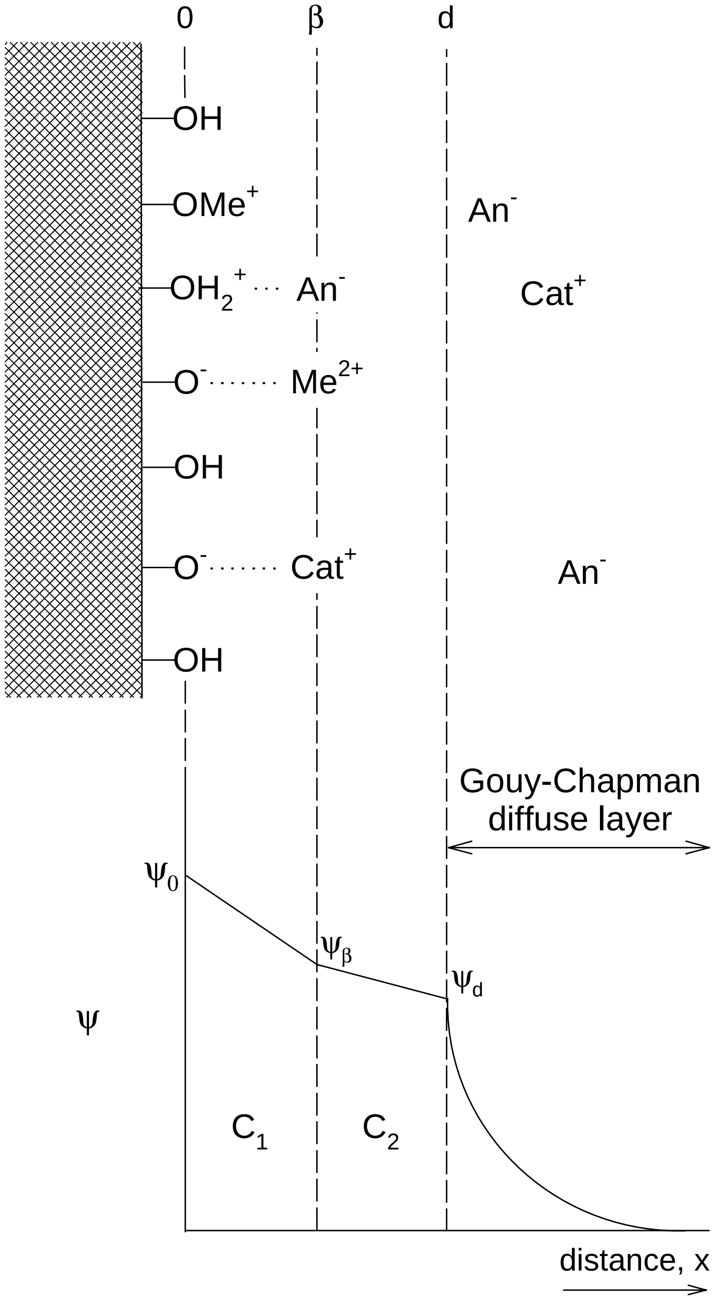

*Figure 6. Potential profile through and location of ions within the electrical double layer according to the triple layer model.*

The triple layer model was introduced to surface complexation studies by Yates et al. (1974) and modified by Hayes and Leckie (1987). In both formulations $H^+$ and $OH^-$ ions enter the innermost layer contributing to the charge $\sigma_0$ and experiencing the potential $\psi_0$. The $\beta$-plane (the inner Helmholtz plane, IHP) is separated from the surface by a region of capacitance $C_1$. Electrolyte ions are assigned to this $\beta$-plane thereby contributing to the charge $\sigma_\beta$ and experiencing the potential $\psi_\beta$. In the Hayes–Leckie modification adsorbing metal ions are allowed to form surface complexes at either the *o*-plane (i.e. inner-sphere complexes) or the $\beta$-plane (i.e. outer-sphere complexes) instead of the $\beta$-plane only as suggested in the original formulation (Yates et al. 1974). The IHP is separated from the *d*-plane (outer Helmholtz plane, OHP) at the potential $\psi_d$ by a region of capacitance $C_2$. As mentioned already above, the *d*-plane represents the distance of the closest approach of completely hydrated non-specifically adsorbed counterions that balance out the charge resulting from the formation of the surface complexes at the *o*- and $\beta$-planes. These non-specifically adsorbed ions are accumulated and distributed by the contrasting action of the electric field and thermal motion in the diffuse layer (extending from the *d*-plane to the bulk of the solution) and contribute to the solution charge with an amount denoted by $\sigma_d$. In some treatments, it is reasonable to locate the charge density $\sigma_d$ at a single plane lying at a specific distance (usually at the *d*-plane) from the surface. However, the potential profile through the diffuse layer, as illustrated in Figure 6, is a consequence of $\sigma_d$ distributed according to the Gouy–Chapman theory. The linear potential profiles between the *o*- and $\beta$-planes as well as between the $\beta$- and *d*-planes result from the placement of the specifically adsorbed ions at the specified planes (*o*- and $\beta$-planes), between which the charge density is zero. The capacitance values $C_1$ and $C_2$ are taken as adjustable parameters, although the evaluation of anion and cation adsorption data could provide the basis for two independent determinations of the capacitance $C_1$, as pointed out by Sposito (1984, pp. 181–182). Because of electroneutrality, the sum of the above mentioned charges is zero:

$$\sigma_o + \sigma_\beta + \sigma_d = 0 \tag{44}$$

These charges are also related to potentials at the various planes according to the equations

$$\sigma_o = C_1(\psi_o - \psi_\beta) \tag{45}$$

$$\sigma_d = C_2(\psi_d - \psi_\beta) \tag{46}$$

Further, in the simplest case of a symmetrical 1–1 electrolyte Gouy–Chapman theory gives the relationship (47) between $\sigma_d$ and the potential $\psi_d$. Frequently, the experimentally accessible zeta potential is taken to be equal to $\psi_d$, although this remains problematic, as pointed out by Wood et al. (1992).

$$\sigma_d = -(8RT\varepsilon\varepsilon_o c)^{½} \sinh (zF\psi_d/2RT) \tag{47}$$

## 3.3 Comparison of the surface complexation models

Above we have shortly discussed three of the most common surface complexation models: the constant capacitance model, the diffuse layer model and the triple layer model. In the constant capacitance and diffuse layer models all specifically adsorbed metals and anions (i.e. those held by non-coulombic forces) are located at the surface plane, as well as are the adsorbed $H^+$ and $OH^-$. These models use a single potential plane on the surface; hence, all specifically adsorbed ions are considered potential-determining and all surface complexation reactions are considered to form inner-sphere complexes. When dealing with these models, the attributes *potential-determining*, *specifically* and *inner-sphere* are, however, not usually mentioned but only implied. These models differ from each other only in the way of treating the completely hydrated non-specifically adsorbed counter-ions that balance out the charge resulting from the formation of surface complexes. This difference is manifested in the different expressions for the interfacial capacitance.

The triple layer model is a more general surface complexation model from which the other models can be derived under specific conditions. When the capacitance between the IHP and OHP, $C_2$, is very large, the triple layer model reduces to the Gouy–Chapman–Stern model, which has been used only in few surface complexation studies (e. g. Fornasiero et al. 1992, Zhang et al. 1995a, b, c). Further, the widely used constant capacitance model may be regarded as the high-ionic-strength limiting case of the Gouy–Chapman–Stern model when also the diffuse layer capacitance is much higher than the compact layer capacitance. It can also be shown that under low-ionic-strength, low-potential conditions the composite capacitance of the interfacial layer (33) will be governed by the diffuse layer capacitance. Hence, under these conditions the Gouy–Chapman–Stern model reduces to the diffuse layer model, also widely used in surface complexation studies.

We would like to point out that the disposition of the ions incorporated into the interfacial region depends on the used model. Before the publication of the paper by Hayes and Leckie (1987), there was actually no need for the terms inner-sphere complex and outer-sphere complex. Unfortunately, the introduction of these concepts has caused some confusion in the use of the generic terms specific adsorption and non-specific adsorption. According to our understanding, the triple layer model presents a more detailed structure of the compact layer and consequently, both inner-sphere and outer-sphere complexes are best characterised as specifically adsorbed ions, while the completely hydrated ions in the diffuse layer are considered non-specifically adsorbed. However, in many papers on triple layer model the term specific adsorption is used only for the inner-sphere complexes, while the outer-sphere complexes are considered non-specifically adsorbed.

The triple layer model has two features which are not a part of the simpler models: the equilibrium constants are applicable over a wide range of ionic strengths and the value $\psi_d$ predicted by this model can be used as an estimate of the electrokinetic potential enabling the use of the experimental zeta potential data in model fitting. Actually, the effect of changing background electrolyte concentration (i.e. changing the ionic strength) on the adsorption behaviour of metal cations is utilized to distinguish between inner- and outer-sphere complex formation. Hayes and Leckie (1987) showed that, in general, modelling results assuming an inner-sphere complex agree well with experimentally observed metal ion adsorption which is relatively unaffected by changing ionic strength conditions. This kind of behaviour is typical for the strongly sorbing divalent transition metal cations (e.g. $Zn^{2+}$ and $Co^{2+}$). Strong dependence of adsorption on ionic strength indicates formation of outer sphere complexes, which is typical for alkaline earth cations (Hayes and Katz 1996). In addition to ionic strength dependence studies, nowadays also direct spectroscopic measurements, especially X-ray absorption spectroscopy, XAS, are increasingly used to distinguish between inner- and outer-sphere complex formation (Hayes and Katz 1996).

## 3.4 Extraction of the parameters

In Chapter 3.2.1 we used the constant capacitance model and the simple system of acid–base reactions (1) and (2) to demonstrate how the intrinsic equilibrium constants and capacitance values can be graphically extrapolated from titration data. Although an extension of such a graphical method can also be used in combination with the triple layer model (Wood et al. 1990, Goldberg 1992) the parameters are usually extracted by a general data fitting procedure utilizing the matrix formulation described above (cf. Chapter 3.1). Nearly always the numerical calculations are carried out by some version of the objective curve-fitting routine FITEQL developed by Westall in the beginning of the 80´s (Westall 1982). Now FITEQL has advanced to version 4.0 (Herbelin and Westall 1999). Below, we illustrate the principles of this procedure using our simple system as an example. By using the constant capacitance model (35) in equation (25) we obtain the required balance equation for the electrostatic component.

$$T_\sigma = (saC_d\,\psi_0)/F = [\equiv\text{Fe–OH}_2^+] - [\equiv\text{Fe–O}^-] \qquad (48)$$

The equilibrium system is now described by the matrix equations (24) and (27) which is a general method of formulating chemical equilibrium problems (Westall 1980). Usually in chemical equilibrium problems, we are given the total (i.e. analytical) concentrations of all components, the stoichiometry and stability constants of all species, and asked to find the free equilibrium concentrations of all components, from which we can easily compute the free concentrations of all species. In these problems, starting from a guess at the free concentrations of components, approximate concentrations of the species are computed using an equation similar to (24). The error, $\boldsymbol{Y}_i$, for each component in the material balance equation (27) can be computed using the approximate concentrations of species:

$$\boldsymbol{Y} = \boldsymbol{A}^t\boldsymbol{C} - \boldsymbol{T} \qquad (49)$$

Using an iterative procedure employing the computed derivative of these errors with respect to the concentration of components an improved guess is computed for the concentration of components. This iteration is carried out until the error in the material balance equation is small compared to the terms in the equation.

In the present case, the equilibrium constants are not known and equations (24) and (49) are used as the basis for optimizing or fitting their values, provided that for some component we have experimental data for both the total concentration, $T_j$, and the free concentration, $X_j$. From these experimental data, usually consisting of titration points, it is possible to find the difference between the total concentration calculated from material balance equation, $T_j^{calc}$, and the directly measured total concentration, $T_j^{exp}$. For example:

$$Y_H = T_H^{calc}\,(T_{\equiv Fe-OH}, T_\sigma, X_H) - T_H^{exp} \qquad (50)$$

Minimization of the sum (over all experimental data points, i.e. titration points, $T_H^{exp}$, $X_H$) of the squares of the values of the differences $Y_H$ with respect to the adjustable parameters is the basis of the optimization procedure. For the surface hydrolysis equilibria discussed above, the only component for which this minimization is possible is $H^+$, for which both pH (or $[H^+]$) and $T_H$ are known. However, the method is general and material balance equation for some other component, e.g. the adsorbing metal, can be used for optimization of parameters as well.

In practise, the procedure to extract the chemical parameters needed to describe an adsorption system consists of several steps, which are clearly summarized by Hayes and Katz (1996). If the protonation constants of the sorbent are not known, the first step is to determine them by conducting acid–base titrations and fitting the data to a reaction model. The actual adsorption modelling is commenced by identifying the number and stoichiometry of the adsorption reactions needed to quantify adequately the experimental adsorption data. In the case of the triple layer model it has also to be decided which reactions are best described as inner-sphere versus outer-sphere adsorption reactions for which purpose spectroscopic and ionic strength dependence studies are used. As a result of an iterative optimisation and refinement process the relevant protonation and adsorption reactions are defined and quantified by intrinsic equilibrium constants. In all of the discussed models, except the diffuse layer model, also values for the interfacial capacitances are obtained in this data fitting procedure. Once the values for intrinsic equilibrium constants and specific capacitance(s) are known, the equations describing the surface reactions can be combined with the conventional mass action and material balance equations for the solution species, to calculate the complete speciation in the total system.

There exists basic agreement that the conceptual model of surface complexation is valid, although appreciable data and experience are needed to exploit effectively surface complexation models. However, because several different implementations of the electrostatic aspects of the surface complexation models are used and each of them represent and calculate the model surface potentials that appear in the exponential coulombic correction factor of the equilibrium constants differently, several sets of surface complexation model constants exist in the adsorption literature. It has been found (e.g. Westall and Hohl 1980) that, especially for data collected at only one ionic strength, several models may perform well in reproducing the experimental data (e.g. the dependence of metal adsorption on pH). Furthermore, all the adjustable parameters may have physically reasonable values, but the values of analogous adjustable parameters differ in different models. Although the values obtained for the adjustable parameters are certainly consistent with the data, they are obviously not the only possible interpretation. This has resulted in a situation where existing data has been interpreted with a variety of surface complexation models which are not consistent with each other in the sense that the parameters are not interchangeable. The situation can be summarized by emphasizing that the chemical species defined and the equilibrium constants obtained with one model must never be used as such in any other model.

Based on the above discussion, it is evident that a separate and self-consistent set of surface acidity and binding constants along with other model parameters must be determined for each sorbent and each version of the surface complexation model. In general such compilations of equilibrium constants, comparable to those available for solution reactions, do not exist. However, in the case of ferrihydrite as the sorbent, Dzombak and Morel (1990) critically analysed all available sorption data and fitted it to the generalized two-layer model to produce a coherent compendium of surface complexation constants for inclusion in chemical equilibrium models. A less comprehensive compilation of surface complexation constants on various sorbents is included in the review by Goldberg (1992). Due to the work of Dzombak and Morel (1990) it is possible to estimate the sorption behaviour of various ions in aqueous ferrihydrite systems based just on chemical analysis of the solution phase without any fitting parameters to site data. As will be shown in Chapter 4.5 we have taken this approach to study the adsorption of zinc and cobalt on iron oxide films.

# 4. Adsorption of cobalt and zinc on ferrihydrite at 25 °C

## 4.1 Surface chemical properties of ferrihydrite

Generally iron oxides have a high energy of crystallization resulting in minute crystals and in a high specific surface area, often >100 $m^2/g$ at which the ≡Fe–OH functional groups are exposed. Consequently, they are effective sorbents for a large range of dissolved ions, molecules and gases. Ferrihydrite is known to form very small particles, a few nanometers in diameter and more or less spherical in shape. However, there is considerable uncertainty about the surface area of ferrihydrite. Thus, its estimated values vary between 100 $m^2/g$ and 700 $m^2/g$ depending on the method and on the source and degree of ordering of the sample (Cornell and Schwertmann 1996, pp. 99–101). A theoretical upper limit of 840 $m^2/g$ is reported by Dzombak and Morel (1990, p. 91) based on the assumption of 2-nm-diameter spheres and a density of 3.57 $g/cm^3$. However, after a critical survey of all literature data, Dzombak and Morel (1990, p. 91) chose the value of 600 $m^2/g$ as the best estimate for ferrihydrite surface area and, consequently, used it in the subsequent calculations.

Dzombak and Morel (1990) also surveyed and synthesized the other available information on the major physical–chemical properties of ferrihydrite in order to obtain the best estimates for the surface properties of ferrihydrite needed in surface complexation modelling. Based on a review of numerous published papers, they found a value of 0.2 mol / mol Fe as the best estimate for the site density of the total reactive sites (i.e. reactive ≡Fe–OH functional surface groups) available for sorption of protons, cations and anions (Dzombak and Morel 1990, p. 94). As discussed earlier, according to the generalized two-layer model, there is a smaller set of high-affinity cation binding sites for which Dzombak and Morel (1990, p. 93) use the value of 0.005 mol / mol Fe as the best estimate. To be able to convert from grams of ferrihydrite per liter of solution to moles of Fe per liter of solution, they assumed the stoichiometry $Fe_2O_3 \cdot H_2O$ which means that 89 g of ferrihydrite contains one mole of Fe (Dzombak and Morel 1990, p. 92). This figure is quite close to the value of 96 g of ferrihydrite containing one mole of Fe, which is obtained assuming the stoichiometry $Fe_5HO_8 \cdot 4\ H_2O$ suggested by Cornell and Schwertmann (1996, p. 2).

Employing a systematic parameter extraction methodology Dzombak and Morel (1990, p. 101) analysed all the published acid–base titration studies on ferrihydrite and found the values $pK_{a1}^{int} = 7.29$ and $pK_{a2}^{int} = 8.93$ be the best estimates for the intrinsic acidity constants (cf. reactions (36) and (37) and equations (38) and(39)). Although we are only seldom interested in these reactions as such, they have to be taken into account in all aqueous adsorption studies on ferrihydrite as cation sorption is dominated by proton competition. It is easy to show that, in the absence of specific cation or anion adsorption, the number of positively and negatively charged sites is equal and the surface is uncharged at a pH halfway between the two acidity constants. The calculated value of this pristine point of zero charge (ppzc), 8.1, is in close agreement with the measured values compiled by Dzombak and Morel (1990, p. 94) and spanning a range from 7.9 to 8.2.

## 4.2 Adsorption data

The classical approach in studying how strongly an aqueous metal ion binds to a particle surface is the wet chemical measurement of the extent to which the adsorbent (solid) removes the adsorbate (dissolved metal) from a solution. The measured data can be used to construct adsorption isotherms showing the amount of adsorbate taken up per unit area of the adsorbent vs. the equilibrium concentration remaining in the solution phase at constant temperature and pH. The adsorption data is often presented on log–log plots, as illustrated for zinc adsorption on ferrihydrite in Figure 7 (the meaning of the solid and dashed lines will be explained later on page 40), and fitted to an adsorption isotherm equation, e.g. the Langmuir or the Freundlich equation. Adsorption of anions on ferrihydrite often obeys the Langmuir isotherm, which on a log–log plot has unit slope at low concentrations and levels off at higher concentrations indicating site saturation. In such a case the proportionality between sorbed and dissolved concentration is linear and the behaviour is consistent with a single type of binding site.

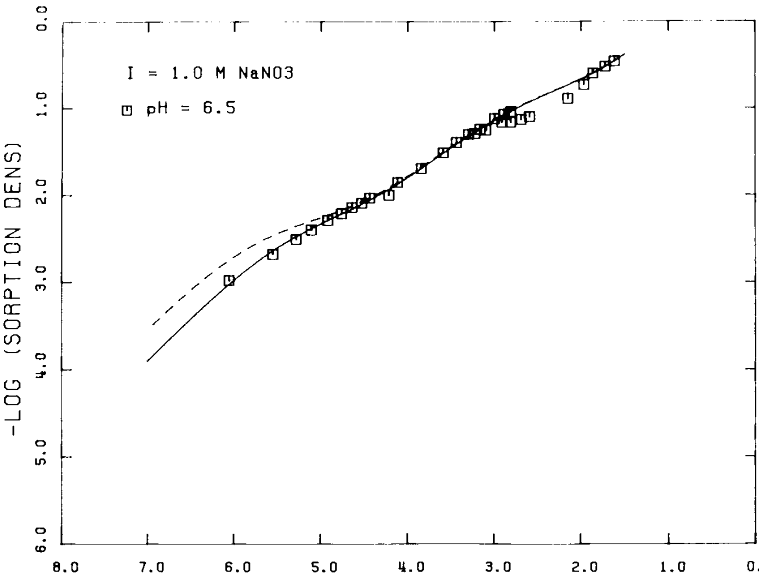

*Figure 7. Zn adsorption isotherm on ferrihydrite measured at pH 6.5. Data of Kinniburgh and Jackson (1982) presented by Dzombak and Morel (1990). The meaning of the solid and dashed lines is explained on page 40.*

In the case of cation adsorption on ferrihydrite, the isotherm often appears linear at low cation concentrations, but follows logarithmic Freundlich slopes in higher concentration ranges. According to Dzombak and Morel (1990, p. 56, 58), this kind of behaviour suggests that the surface is composed of many groups of binding sites with varying strength of binding between the metal and the surface site. Although the Freundlich equation giving the relationship $\Gamma_x = kc^{1/n}$ between the adsorbed amount $\Gamma_x$ and the equilibrium concentration in solution, $c$, and corresponding to straight lines with slopes less than 1 on log–log graphs, is convenient for representing data, it is purely empirical containing two adjustable parameters, $k$ and $n$. At high sorbate–sorbent ratios also surface precipitation may participitate in the total apparent sorption of cations. This surface precipitation of metal hydroxides is known to take place at lower pH values than bulk precipitation and, consequently, the removal of metals from solution by adsorption and precipitation cannot always be clearly separated. In a log–log plot such a behaviour is manifested by a smooth but rapid increase in sorption density with increasing sorbate concentration and a smooth transition between surface reactions and bulk solution precipitation as seen also in Figure 7.

Sorption of both cations and anions on ferrihydrite is strongly dependent on pH. Because of the strong influence of pH, in addition to the log–log isotherms discussed above, the sorption data obtained at constant sorbate and sorbent concentrations are commonly presented in plots of percent sorbed versus pH, referred to as pH edges, as illustrated for zinc sorption on ferrihydrite in Figure 8. The trend shown in this figure (increasing uptake with increasing pH until a plateau at 100% is reached) is typical of cation adsorption on metal oxides. Adsorption increases from hardly measurable values to almost 100% of the amount added over a narrow region of 1–2 pH units termed the adsorption edge. Further, as the sorbate–sorbent ratio is increased above some threshold level, cation adsorption edges shift to the right, which indicates a multiplicity of site types (Dzombak and Morel, 1990, p. 58). As seen in Figure 8, it is obvious that in the case of Zn adsorption on ferrihydrite having total surface Fe concentration of $9.33 \cdot 10^{-2}$ M the treshold Zn concentration is between $1 \cdot 10^{-5}$ M and $1 \cdot 10^{-4}$ M, i.e. the fractional adsorption at a given pH is reduced, when the equilibrium Zn concentration increases from $1 \cdot 10^{-5}$ M to $1 \cdot 10^{-4}$ M. By comparing the position of the adsorption edges of different cations determined at the same sorbate–sorbent ratio, a qualitative assessment of the relative adsorption strengths can be made. The higher the pH of the adsorption edge, the weaker the cation binds to the surface. Results of adsorption studies of various cations on hematite and goethite are clearly summarised by McKenzie (1980) (cited by Cornell and Scwertmann 1990, p. 257) in series of parallel pH edges showing the strength of metal adsorption on hematite to be Pb > Cu > Zn > Co > Ni > Mn. In a similar way, by comparing the data in Figure 8 and Figure 9, we notice that zinc adsorbs more strongly on ferrihydrite than cobalt.

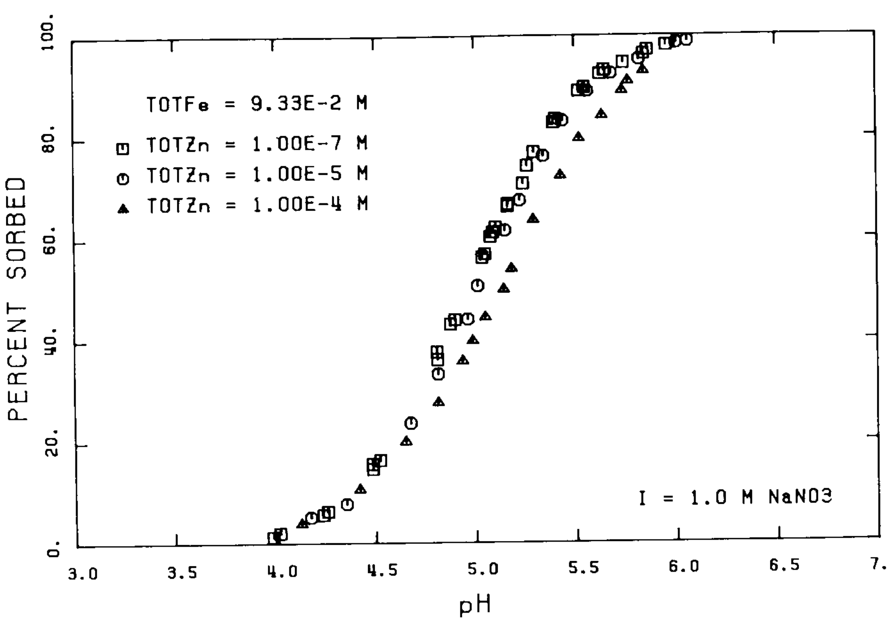

*Figure 8. pH edges for sorption of zinc on ferrihydrite. Data of Kinniburgh and Jackson (1982) presented by Dzombak and Morel (1990).*

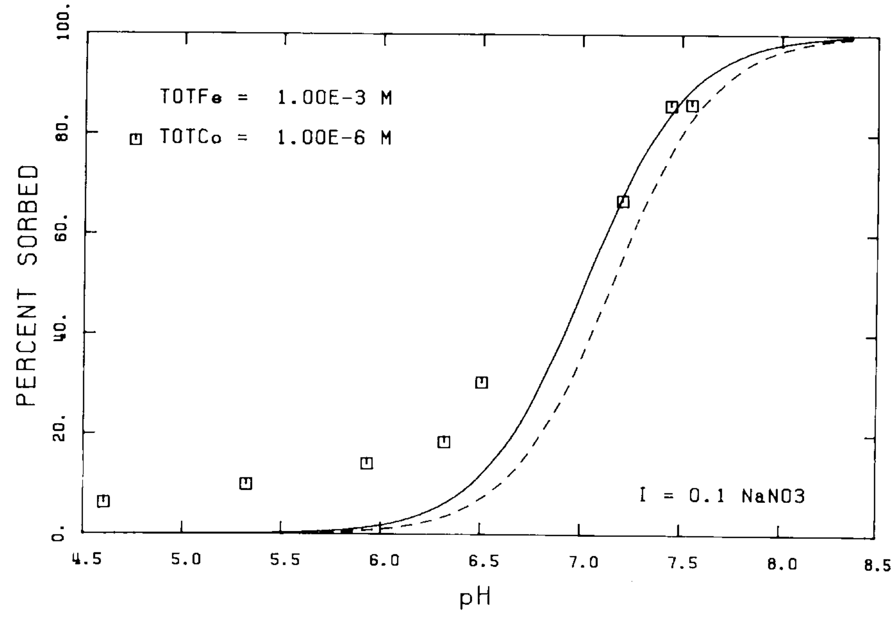

*Figure 9. pH edges for sorption of cobalt on ferrihydrite. Data of Benjamin and Bloom (1981) presented by Dzombak and Morel (1990). The meaning of the solid and dashed lines is explained on page 40.*

## 4.3 Adsorption models

Although the traditional Langmuir and Freundlich isotherms are useful for summarising adsorption data and for comparative purposes, they provide no information about the adsorption mechanism nor about the speciation on the surfaces. Before the breakthrough of the surface complexation models, several models were forwarded to describe e.g. the strong pH dependence of the adsorption of hydrolyzable metal ions (see e.g. the discussion by James, Stiglich and Healy 1975). It was observed that there is a general qualitative relationship between the pH of the adsorption edge and the pH of the hydrolysis of the metal cation in solution. As the first hydrolysis constant of the metal cation in solution rises, the pH of the adsorption edge decreases. This observation was often interpreted in the way that the hydrolysed metal ions, e.g. $Co(OH)^+$ and $Zn(OH)^+$, adsorb preferably to the free metal ions, although the metal uptake often occurs from solutions whose pH values are such that only a small fraction of the total aqueous metal is in the form of soluble hydroxo-metal complex.

Nowadays, adsorption on oxide surfaces is usually treated by means of the surface complexation models. In a recent review on the surface chemistry of metal oxides, Brown et al. (1999, p. 123) classify the various contributions to the free energy of sorption as follows: 1) the bond energy of sorption; 2) long-range electrostatic attraction to charged surfaces; 3) hydrophobic bonding and the energy contributions due to the changes in the extend and structure of hydration of both the surface and adion; and 4) the energy involved in protonation–deprotonation of the sorption sites and hydrolysis of the adion (either before or during sorption or precipitation). In the surface complexation models all these contributions are taken into account. Especially, there is no need to invoke hydrolysed species in an explicit way, because the surface complexation equilibria and the hydrolysis–adsorption sequence is indistinguishable as pointed out by Cornell and Schwertmann (1996, p. 257). It is also worthy of note that the adsorption edges for both Zn and Co sorption on ferrihydrite (Figure 8, Figure 9) are observed at pH values lower than the ppzc, 7.9–8.2 (cf. p. 36). This means that Co and Zn are sorbing even though long-range electrostatic forces are repulsive, which means that free energy contributions from 1), 3) and 4) are significantly stronger than that from long-range repulsive forces. As described earlier in this report, the surface complexation models represent adsorption in terms of interaction of the adsorbate with the surface OH groups of the adsorbent oxide. Consequently, fitting the experimental adsorption data, e.g. isotherms or pH edges, to these models, provides information about binding constants and speciation of surface complexes.

### 4.3.1 Work of Dzombak and Morel

As mentioned earlier, Dzombak and Morel (1990) reviewed all the available English language scientific literature on surface properties of and sorption on ferrihydrite. In the case of Co adsorption on ferrihydrite, data from four papers (Kurbatov et al. 1951, Duval and Kurbatov 1952, Benjamin and Bloom 1981, Sipalo-Zulijevic and Wolf 1973) were found reliable enough to be used in the model fitting, while in the case of Zn adsorption, data from six papers (Kinniburgh and Jackson 1982, Benjamin 1978, Kinniburgh et al. 1977 [not available for us], Dempsey and Singer 1980, Leckie et al. 1980 [not available for us]) were used. As there existed only little, if any, spectroscopic data on the structures of the surface complexes, Dzombak and Morel (1990, pp. 82–83) hypothesized simple, chemically reasonable one-to-one surface complexes and tried to fit all the available data with a minimum number of surface species using the generalized double layer model (c.f. Chapter 3.2.2). In this model, cation sorption is represented by reactions (51) and (52) as surface complexation on two site types (weak and strong binding sites denoted by the superscripts w and s) with surface precipitation at high cation concentrations. However, in this work we are interested in the low concentration range and consequently, the discussion of surface precipitation is omitted from the following. Along with the adsorption reactions (51–52) and the deprotonation reactions of the surface hydroxyl groups (36–37), the "known" solution complexation reactions (14, 53–55) were considered by Dzombak and Morel, when they modelled Zn adsorption on ferrihydrite.

$$\equiv Fe^{s}OH + Zn^{2+} = \equiv Fe^{s}OZn^{+} + H^{+} \qquad K_1 \tag{51}$$

$$\equiv Fe^{w}OH + Zn^{2+} = \equiv Fe^{w}OZn^{+} + H^{+} \qquad K_2 \tag{52}$$

$$Zn^{2+} + OH^{-} = ZnOH^{+} \tag{53}$$

$$Zn^{2+} + 2OH^{-} = Zn(OH)_2(aq) \tag{54}$$

$$Zn^{2+} + 3OH^{-} = Zn(OH)_3^{-} \tag{55}$$

Using the FITEQL program and the above reactions, Dzombak and Morel (1990, pp. 111–113) extracted optimal surface complexation constants, $K_1^{int}$ and $K_2^{int}$, separately from each individual Zn adsorption data set. The way how this can be done with the latest FITEQL version, 4.0, employing adsorption edge data is clearly demonstrated in an example problem presented in the FITEQL manual (Herbelin and Westall, 1999, pp. 6–14…6–16). In addition to the numerical values of the intrinsic constants, Dzombak and Morel (1990, pp. 113–123) present the results as plots showing the original data along with pH edges or adsorption isotherms calculated according to the established model (cf. Figure 7 and Figure 9). The solid lines in these figures represent the optimal fits to the particular data sets, while the dashed lines correspond to the best overall estimate of the surface complexation constants. The best overall estimates for the Zn surface complexation constants on ferrihydrite were calculated by a weighted average of optimum $\log K^{int}$ values for each individual data set. This issue of choosing the best estimate for an equilibrium constant given a wide range of estimates was addressed for the first time in a systematic way in the work of Dzombak and Morel (1990, pp. 83–86). As seen also in Figure 7, Dzombak and Morel (1990) achieved generally good fits, when they fitted the Zn sorption data, while the results obtained in the case of Co sorption seem to be less than perfect as illustrated in Figure 9. As a result of the parameter extraction and optimisation process, they present the following best estimates for the Zn and Co surface complexation constants on ferrihydrite:

$$\equiv Fe^{s}OH + Zn^{2+} = \equiv Fe^{s}OZn^{+} + H^{+} \qquad \log K_1^{int} = 0.99 \qquad (56)$$

$$\equiv Fe^{w}OH + Zn^{2+} = \equiv Fe^{w}OZn^{+} + H^{+} \qquad \log K_2^{int} = -1.99 \qquad (57)$$

$$\equiv Fe^{s}OH + Co^{2+} = \equiv Fe^{s}OCo^{+} + H^{+} \qquad \log K_1^{int} = -0.46 \qquad (58)$$

$$\equiv Fe^{w}OH + Co^{2+} = \equiv Fe^{w}OCo^{+} + H^{+} \qquad \log K_2^{int} = -3.01 \qquad (59)$$

According to reactions (56–59), cation adsorption is accompanied by a release of protons, which is also a well-known experimental fact providing qualitative support for the representation of surface sites as complexing weak acids. However, the reported values of proton release in the literature cannot be directly equated to a specific reaction stoichiometry. This non-intuitive result of the calculations carried out by Dzombak and Morel (1990, pp. 287–290) on Zn adsorption on ferrihydrite and Hayes (1987, pp. 125–126) on Pb adsorption on goethite points out to the importance of accounting for the redistribution of other surface species during the adsorption process. Indeed, the net release of 1.7 moles of $H^+$ for 1 mole of adsorbed $Zn^{2+}$ on ferrihydrite observed by Kinniburgh (1983) is in close agreement with the value calculated by Dzombak and Morel (1990), who used the generalized two layer model consisting of reactions (36, 37, 14, 51–55).

The experimentally observed correlation between the first hydrolysis constant of cations in solution and the uptake on oxides reflects the affinity of the metals for the oxygen atoms. Cation sorption is analogous to cation hydrolysis in solution in that both processes involve the release of protons and formation of inner sphere complexes between cations and oxygen atoms. This analogy is manifested in the linearity of the plots presenting the logarithmic surface complexation constants against the logarithmic first hydrolysis constants for various cations. These relationships were utilized by Dzombak and Morel (1990, pp. 303–305) to predict surface complexation constants for cations for which no sorption data exist.

## 4.4 Solution equilibria and competitive adsorption

The sorption constants given by Dzombak and Morel (1990) are extracted from equilibrium, single solute sorption data. Background electrolytes are used to fix ionic strength in sorption experiments, but their adsorption is deliberately not considered in the generalized two-layer model. Therefore, Dzombak and Morel (1990, pp. 66, 68) accepted only data obtained in the nitrate, chloride or perchlorate electrolytes, because the monovalent ions $K^+$, $Na^+$, $NH_4^+$, $Cl^-$, $NO_3^-$ and $ClO_4^-$, which originate from these electrolytes can be considered inert, i.e. nonsorbing. Although inert in the sense of sorption, the background electrolyte ions can participitate in solution reactions producing complexes, e.g. $CoCl^+$, which along with the various OH complexes, such as $CoOH^+$, $Co(OH)_2$ and $Co(OH)_3^-$, were taken into account in fitting the sorption data (Dzombak and Morel 1990, pp. 103–105). The other complexing ligands, eventually present in the systems to be modelled, are taken into account by the known solution complexation constants and they may inhibit the adsorption by holding the metal cation as a complex in solution as illustrated in the examples given by Cornell and Schwertmann (1996, p. 260).

The application of the surface complexation models (equilibrium constants) determined for the different single-metal ion–oxide systems to describe sorption in multi-solute systems has received only limited attention. In these systems various ions, e.g. $Co^{2+}$ and $Zn^{2+}$, may compete with each other for adsorption sites. In principle, such a competition is implicitly taken into account in the surface complexation models as 1) differences in the intrinsic stability constants and 2) changes in the electrostatic repulsion due to the adsorption of other charged species. Although Dzombak and Morel (1990, p. 248) do not present any calculations on multi-solute problems, they emphasize the similarity to single-solute calculations, except the greater number of equations involved. In spite of these general facts, some authors consider that surface complexation models do not take into account the competitive interactions. Smith et al. (1998), for example, consider that they have ignored the competitive interactions in their approach to model real-world acid mine drainage systems using chemical analyses of the water and the generalized double layer model without any fitting of parameters to the site data.

Few studies have been performed to compare the experimental metal uptake data in multi-solute systems with the predicted values based upon the surface complexation models for the corresponding single-metal ion systems. Probably the best of these studies has recently been carried out by Palmqvist et al. (1999), who investigated the competitive adsorption of copper, zinc and lead on goethite employing the constant capacitance model. They compared experimental metal uptake and proton stoichiometry results in the multi-metal systems with predicted values based upon surface complexation models for the single-metal systems. It was found that the equilibrium models for the single-metal complexation predicted the speciation accurately also in two-metal-ion systems. Although these results were obtained in specific sorbent–sorbate systems employing the constant capacitance model, they give strong experimental support to the general assumption presented above; surface complexation models for the individual metal ions are combinatory. Palmqvist et al. (1999) present also interesting, although expected, results of calculations in a system where all three metals are present in equimolar concentrations, at a total metal ion concentration corresponding to near saturation of surface sites. These calculations show that the shift in the adsorption edge (compared to the single-metal system) toward higher pH is most significant for the weakest bound metal, zinc. The adsorption of the strongest bound metal, copper, is significantly less influenced by the competition than those of lead and zinc. On the other hand, in cases with a large excess of active surface sites over metal ions, the effect of competition is negligible.

The competitive adsorption of zinc and cobalt on ferrihydrite is mentioned in a paper by Benjamin and Leckie (1981). Regretfully, no results on this system are shown, but it is only mentioned that the results are similar to the copper–lead system, where the competitive interactions at low sorbate–sorbent ratios were found to be weak. To explain their results, Benjamin and Leckie (1981) proposed that there are various groups of sites on the ferrihydrite surface having different relative binding strengths for different metals. This leads to much weaker competitive effects than one would otherwise expect. Although, the treatment in this often cited paper is reasonable, interesting and well presented, it seems somewhat outdated as the competition is implicitly taken into account in the surface complexation models.

## 4.5 Simulation of $Co^{2+}$ and $Zn^{2+}$ adsorption on cooling pipe surfaces at 25 °C

In this chapter, we use the generalized two-layer model together with the surface complexation reactions and associated equilibrium constants proposed by Dzombak and Morel (1990) (cf. Chapters 4.1 and 4.3.1) to study the adsorption of zinc and cobalt on ferrihydrite. Combining the information on these reactions with knowledge on physical characteristics of the cooling system and chemical analyses of the coolant, we simulate the competitive effect of zinc addition on cobalt adsorption on oxide films formed on material surfaces in the primary circuits in nuclear power plants. Otherwise relevant plant data and reasonable assumptions (e.g. the very outermost layer of the film consisting of ferrihydrite) are employed, except the temperature, which in these first adsorption simulations is taken to be 25 °C. The reason for this is, that systematised adsorption data at elevated temperatures is not easily available.

### 4.5.1 Characterisation of the adsorption system

In the following calculations we study the adsorption in a one meter long piece of a cooling pipe having an inner diameter of 35 cm. Adsorption is assumed to take place in a 0.6 μm thick outermost layer of the oxide film consisting of ferrihydrite. The properties of ferrihydrite needed in the characterisation of the adsorption system are taken from Dzombak and Morel (1990), discussed in Chapter 4.1 and summarised in

Table 2. Figure 10 illustrates how this data is used to calculate the parameters needed in the surface complexation model.

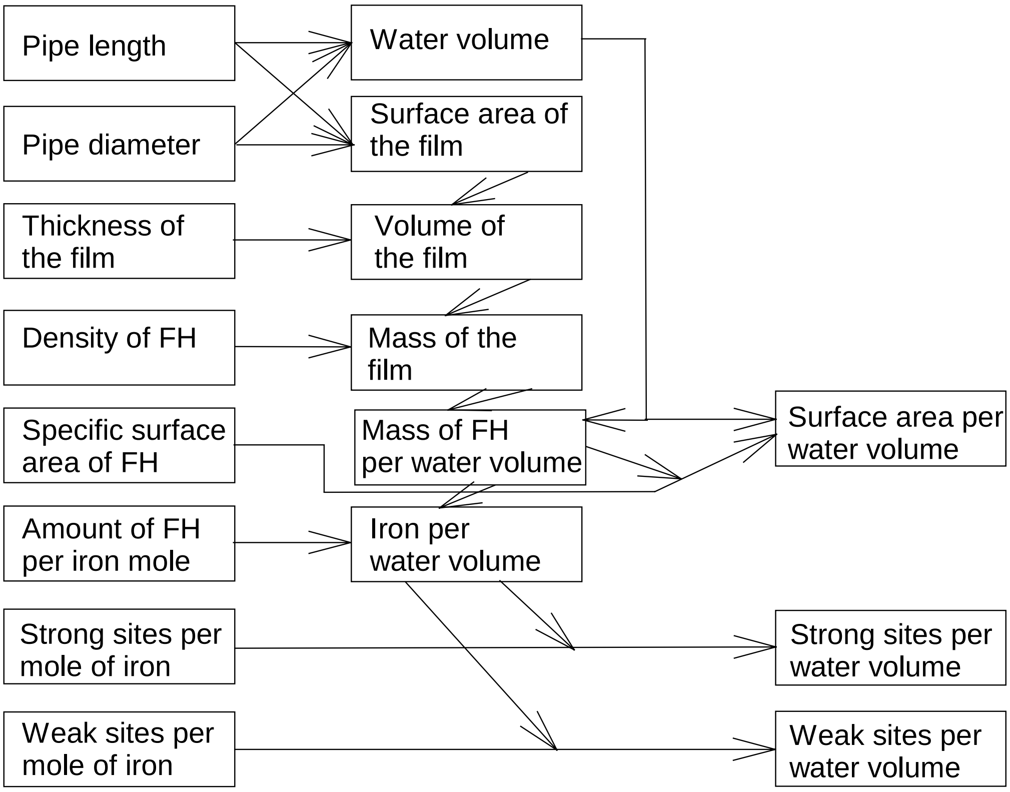

*Figure 10. Calculation of the parameters needed in the surface complexation model. Ferrihydrite is abbreviated by FH.*

*Table 2. Characteristics of the adsorption system.*

| | |
|---|---|
| Physical dimensions | |
| length of the pipe | 1 m |
| inner diameter of the pipe | 0.35 m |
| thickness of the film | 0.6 μm |
| water volume | 96 l |
| Properties of ferrihydrite (from Dzombak and Morel 1990) | |
| density | 3570 kg $m^{-3}$ |
| specific surface area | 600 $m^2$/g |
| mass of ferrihydrite per one mole of Fe | 89 g/mol |
| density of strong adsorption sites | 0.005 mol / mol Fe |
| density of weak adsorption sites | 0.2 mol / mol Fe |
| Calculated properties of the oxide film | |
| surface area of the film | 1.1 $m^2$ |
| volume of the film | $6.6 \cdot 10^{-6}$ $m^3$ |
| mass of the film | 2.4 g |
| mass of ferrihydrite per water volume | 0.024 g/l |
| amount of Fe in the film per water volume | $0.275 \cdot 10^{-3}$ mol/l |
| Calculated values needed in the surface complexation model | |
| film surface area per water volume | 14.7 $m^2$ / l |
| amount of strong adsorption sites per water volume | $1.4 \cdot 10^{-6}$ mol/l |
| amount of weak adsorption sites per water volume | $55 \cdot 10^{-6}$ mol/l |

### 4.5.2 Adsorption calculations

The behaviour of zinc and cobalt in the above described system is modelled using HYDRAQL software (Papelis et al. 1988) designed especially for modelling adsorption by the surface complexation approach. The considered surface reactions are discussed in Chapters 4.1 and 4.3.1 and briefly summarised with associated equilibrium constants in Table 3.

*Table 3. The considered surface reactions with associated intrinsic equilibrium constants.*

| | |
|---|---|
| $\equiv Fe–OH_2^+ = \equiv Fe–OH + H^+$ | $\log K_{a1}^{int} = –7.29$ |
| $\equiv Fe–OH = \equiv Fe–O^- + H^+$ | $\log K_{a2}^{int} = –8.93$ |
| $\equiv Fe^sOH + Zn^{2+} = \equiv Fe^sOZn^+ + H^+$ | $\log K_{1Zn}^{int} = 0.99$ |
| $\equiv Fe^wOH + Zn^{2+} = \equiv Fe^wOZn^+ + H^+$ | $\log K_{2Zn}^{int} = –1.99$ |
| $\equiv Fe^sOH + Co^{2+} = \equiv Fe^sOCo^+ + H^+$ | $\log K_{1Co}^{int} = –0.46$ |
| $\equiv Fe^wOH + Co^{2+} = \equiv Fe^wOCo^+ + H^+$ | $\log K_{2Co}^{int} = –3.01$ |

In Figure 11 we present simulated adsorption edges of zinc in the presence of a minute amount of cobalt. As expected (cf. Chapter 4.2), the adsorption edges shift to the right as the sorbate–sorbent ratio, i.e. the total amount of zinc (the sum of dissolved and adsorbed amounts), increases. Similar adsorption edges for cobalt are presented in Figure 12. Compared to zinc, cobalt adsorption edges are obtained at higher pH values reflecting the weaker binding of cobalt to ferrihydrite which is evident also by comparing the values of the intrinsic equilibrium constants given in Table 3.

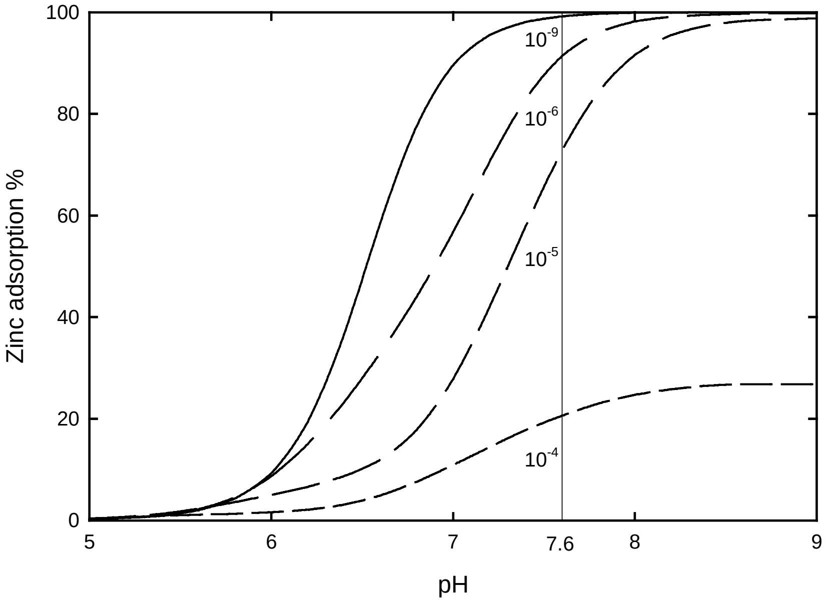

*Figure 11. Simulated zinc adsorption edges on ferrihydrite in the presence of a minute amount ($10^{-12}$ M) of cobalt. The total concentration of adsorption sites is $5.6 \cdot 10^{-5}$ M and the total zinc concentration varies from $10^{-9}$ M to $10^{-4}$ M as indicated on the adsorption edges. pH 7.6 is indicated by the vertical line to assist comparisons between Figures 11–14.*

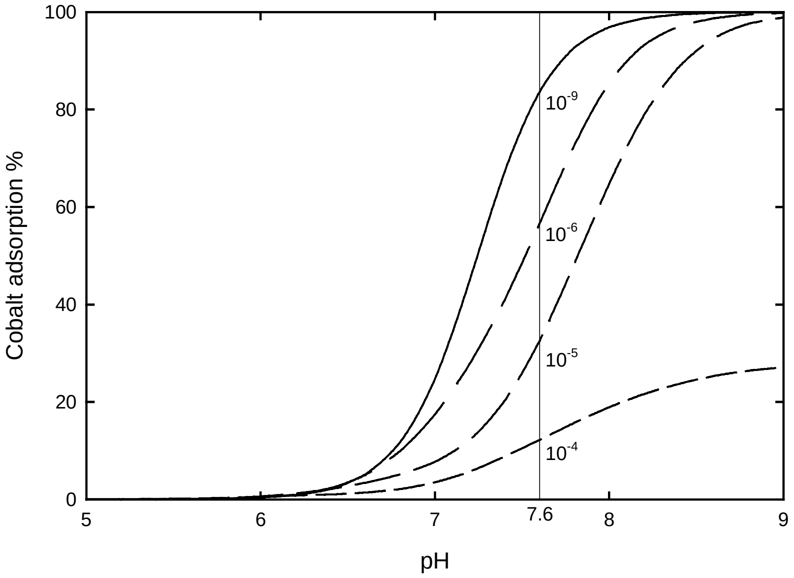

*Figure 12. Simulated cobalt adsorption edges on ferrihydrite in the presence of a minute amount ($10^{-12}$ M) of zinc. The total concentration of adsorption sites is $5.6\cdot10^{-5}$ M and the total cobalt concentration varies from $10^{-9}$ M to $10^{-4}$ M as indicated on the adsorption edges. pH 7.6 is indicated by the vertical line to assist comparisons between Figures 11–14.*

In Figure 13 we illustrate the competitive effect of zinc addition on cobalt adsorption. The total cobalt concentration (i.e., the sum of dissolved and adsorbed amounts of cobalt divided by the solution volume) in these simulations is taken as $5\cdot10^{-9}$ M (0.3 ppb). The values on the *y* axis give the adsorbed fraction of cobalt as a function of solution pH. Changing the total zinc concentration from $1\cdot10^{-10}$ M (0.007 ppb) to $1\cdot10^{-7}$ M (7 ppb) already leads to a situation in which the more strongly binding zinc retards cobalt adsorption. The latter concentration is in the range of Zn concentrations in the reactor water of plants which are dosing Zn (Mäkelä et al. 1999). At pH 7.6 (indicated by the vertical line) the addition of $1\cdot10^{-5}$ M (700 ppb) zinc results in the reduction of cobalt adsorption from 80% to 20% on the oxide surface.

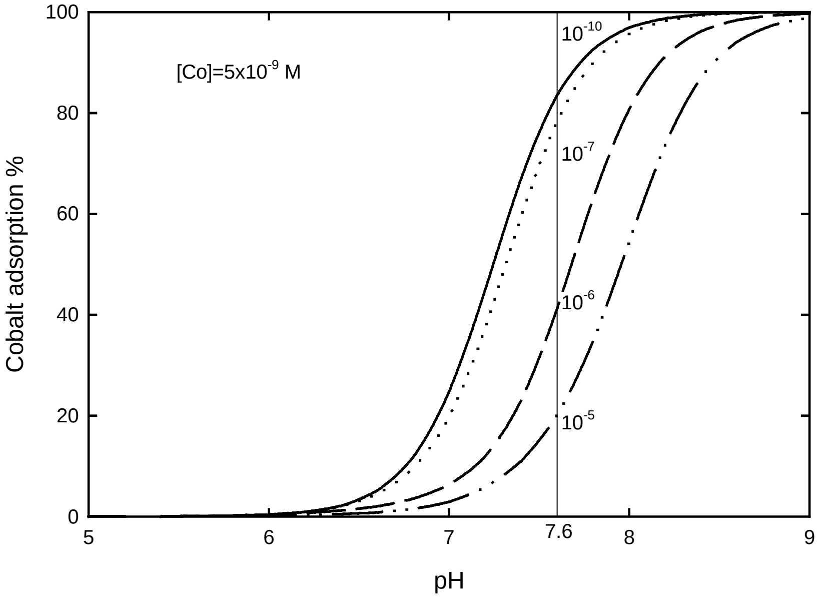

*Figure 13. The effect of increasing zinc concentration (from $10^{-10}$ M to $10^{-5}$ M, i.e. from 0.007 ppb to 700 ppb) on the adsorption of cobalt at 25 °C on ferrihydrite from water containing $5 \cdot 10^{-9}$ M (0.3 ppb) cobalt. The total concentration of adsorption sites is $5.6 \cdot 10^{-5}$ M. pH 7.6 is indicated by the vertical line to assist comparisons between Figures 11–14.*

From 14, it can be seen that the more weakly binding cobalt has only a minor retarding effect on zinc adsorption even at a total cobalt concentration of $10^{-6}$ M. First when the total cobalt concentration approaches the concentration of adsorption sites, zinc adsorption is significantly retarded.

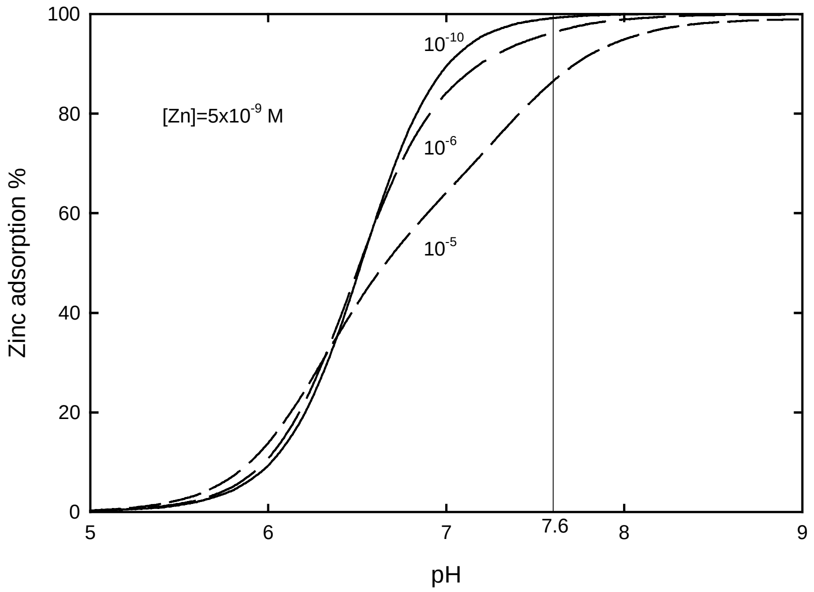

*Figure 14. The effect of increasing cobalt concentration (from $10^{-10}$ M to $10^{-5}$ M) on the adsorption of zinc at 25 °C on ferrihydrite from water containing $5{\cdot}10^{-9}$ M zinc. The total concentration of adsorption sites is $5.6{\cdot}10^{-5}$ M. pH 7.6 is indicated by the vertical line to assist comparisons between Figures 11–14.*

In Figure 15 we present tentative results of a somewhat different calculation simulating the conditions where dissolved zinc and cobalt concentrations in the coolant are $0.3{\cdot}10^{-9}$ M (0.02 ppb) and $0.5{\cdot}10^{-9}$ M (0.03 ppb), respectively. These concentrations roughly correspond to those analysed from some BWR coolants. The calculations indicate that such solution concentrations and an equilibrium pH of 8.2 are achieved in *Case 1*, where the total zinc and cobalt concentrations are $2{\cdot}10^{-7}$ M and $18{\cdot}10^{-9}$ M, respectively. A three-fold increase in the total zinc concentration (to $6{\cdot}10^{-7}$ M) in *Case 2* results in a ten-fold increase in the dissolved zinc concentration ($3{\cdot}10^{-9}$ M, 0.2 ppb) at pH 8.2. Simultaneously, the total (and adsorbed) cobalt concentration corresponding to an unchanged dissolved cobalt concentration of $0.5{\cdot}10^{-9}$ M (0.03 ppb) is reduced by more than 50% (to $8{\cdot}10^{-9}$ M) compared to *Case 1*. As the general trend is, that an increase in the temperature of the system promotes significantly cation uptake (cf. the discussion in Chapter 5.5), we expect that at elevated temperatures similar results are obtained at considerable lower pH values.

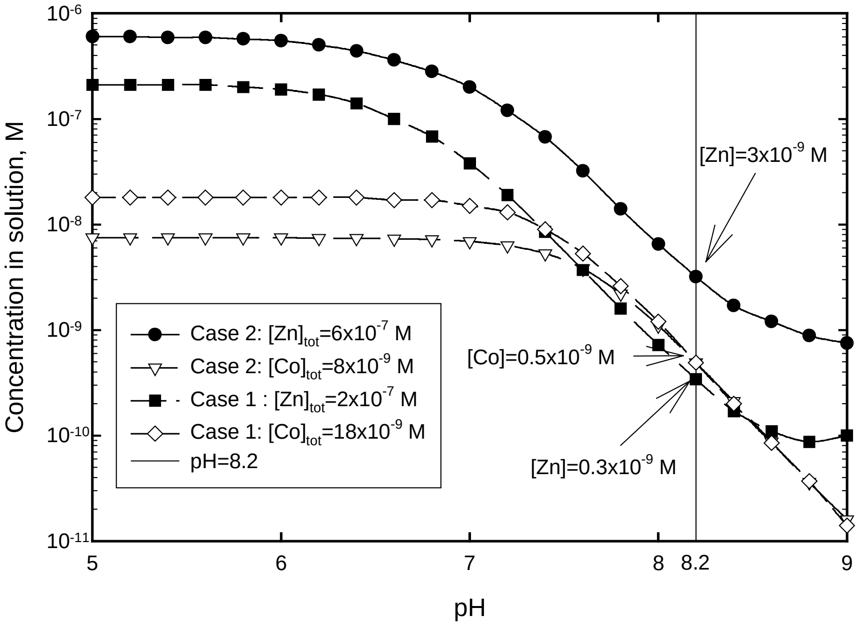

*Figure 15. Solution concentrations of zinc and cobalt as a function of pH in two cases of competitive adsorption on ferrihydrite. In Case 1 the total zinc concentration is $2 \cdot 10^{-7}$ M and the total cobalt concentration $18 \cdot 10^{-9}$ M. In Case 2 the dissolved cobalt concentration at pH 8.2 is required to remain unchanged ($0.5 \cdot 10^{-9}$ M) and the total zinc concentration is increased three-fold (to $6 \cdot 10^{-7}$ M). As a consequence of the increased zinc concentration, the total (and adsorbed) cobalt concentration is reduced by more than 50 % compared to Case 1.*

# 5. Effect of elevated temperature on surface complexation on iron oxides

In addition to pH, sorbent–sorbate ratio, competition and ionic strength discussed above, also temperature can profoundly influence ion adsorption, and, in fact, the influence of temperature can approach that of pH in affecting adsorption behaviour. In addition to technological systems, such as the corrosion phenomena in nuclear power plants, adsorption processes are important in a wide temperature range also in soil and groundwater. This is particularly the case in the final repositories of radioactive waste, where elevated temperatures can be expected due to remaining nuclear fission reactions. However, studies at other than room temperature are rare, and for temperatures above 100 °C the pioneering adsorption studies have been published first in the recent past.

Interpreting adsorption phenomena at elevated temperatures in terms of the surface complexation models requires information on the temperature dependence of the equilibrium constants of the surface and solution reactions. In the case of solution reactions, such information is available, at least to some extent. The effect of temperature on the acid–base reactions of iron oxide surfaces has been investigated in a few studies since the mid 1980´s, but the first papers explaining the effect of temperature on metal adsorption on iron oxides by means of rigorous surface complexation models have just come out (Karasyova et al. 1999; Angove et al. 1999). A few calorimetric studies of the oxide–water interface have been conducted at 25 °C to derive enthalpies of surface protonation during acid–base titrations (Machesky and Anderson 1986; de Keizer et al. 1990). Acid–base titrations at different temperatures (usually below 90 °C) have also been performed to estimate surface protolysis enthalpy and entropy values (Blesa et al. 1984; Karasyova et al. 1999; Angove et al. 1999). However, only one research group seems to be able to perform potentiometric acid–base titrations at temperatures above 100 °C (Machesky et al. 1994, 1998a, 1998b; Ridley et al. 1999; Wesolowski et al. 2000). In some studies the focus has been on the temperature dependence of the point of zero charge, which has been related to the enthalpy change of proton adsorption employing sophisticated thermodynamic analyses (Bérubé and de Bruyn 1968; Tewari and McLean 1972; Lyklema 1987; Fokkink et al. 1989). As a result of these studies, few model-dependent enthalpy and entropy values of surface protonation on magnetite, hematite, goethite and rutile are known, along with corresponding quantities for cobalt sorption on goethite. The only reported heat capacities of surface protonation come from the studies on rutile by Machesky et al. (1994, 1998a) and magnetite by Wesolowski et al. (2000).

As the surface complexation properties of ferrihydrite have not been studied over an extended range of temperatures, we will below shortly discuss such studies on the other iron oxides: magnetite (Tewari and McLean 1972; Blesa et al. 1984; Wesolowski et al.

2000), goethite (Machesky and Anderson 1986; Angove et al. 1999) and hematite (Fokkink et al. 1989; de Keizer et al. 1990; Karasyova et al. 1999). Due to its insolubility and redox insensitivity, rutile, $TiO_2$, has been used as a model oxide in several pioneering adsorption studies and, consequently, some pioneering papers dealing exclusively with adsorption on rutile are included in the following discussion (Machesky et al. 1994, 1998a, 1998b; Ridley et al. 1999; Bérubé and de Bruyn 1968). The earlier studies concerning the near room temperatures on ion adsorption on oxides have been reviewed and analysed by Blesa et al. (1990), Machesky (1990), Barrow (1992) and Schoonen (1994). Schoonen (1994) also extrapolated the available (T< 95 °C) point of zero charge data for several oxides to 350 °C, but warned that the uncertainty in these extrapolations increases rapidly above 150 °C, because experimental data were unavailable. As is obvious from the discussion above, several experimental techniques have been employed in the measurements. Similarly, model-dependent quantities called enthalpy and entropy of adsorption of protons (or a similar terminology) have been determined from a number of theoretical interpretations. The selection of the best thermodynamic values for our purposes is not a straightforward task and will be discussed in a subsequent report. Here we confine us to a short qualitative discussion of the key papers.

## 5.1 Temperature dependence of the point of zero charge

The generic term for the pH at which a metal oxide in contact with an aqueous solution has no net surface charge is the point of zero charge, $pH_{pzc}$. In the absence of specific binding of solution ions other than $H^+$ and $OH^-$, the overall surface charge is exactly balanced by protonated and deprotonated surface sites at this point, i.e., according to the model represented by equations (36) and (37) $[\equiv FeO^-] = [\equiv FeOH_2^+]$. This condition can be termed the pristine point of zero charge, $pH_{ppzc}$, which according to the same model is equal to $(pK_{a1}^{int}+pK_{a2}^{int})/2$. In most of the studies considered below, the $pH_{ppzc}$ has been evaluated by determining the point of intersection of a series of acid–base titration curves obtained at various inert background electrolyte concentrations, $pH_{cip}$ (= pH of the <u>c</u>ommon <u>i</u>ntersection <u>p</u>oint). Generally, the increase of the electrolyte concentration results in a greater net $H^+$ and $OH^-$ adsorption because counterions more effectively screen the resulting surface charge. Only at the $pH_{ppzc}$, this effect is absent, because the net surface charge is zero and, consequently, all the titration curves intersect. However, in the presence of other specifically adsorbing ions, the $pH_{cip}$ values differ in a predictable way from the $pH_{pzc}$ and the $pH_{ppzc}$ values (Lyklema 1987). In the studies considered below, the absence of specific adsorption is usually assumed and, hence, the equality of the $pH_{pzc}$, $pH_{ppzc}$ and $pH_{cip}$ is implied and the term "point of zero charge" used. Only in the paper by Wesolowski et al. (2000), it is important to explicitly distinguish between these concepts.

The influence of temperature on the metal oxide–water interface was first studied by Bérubé and de Bruyn (1968) who described the temperature dependence of the point of zero charge of rutile in terms of thermodynamic magnitudes for the adsorption of $H^+$ and $OH^-$ ions. Following this line, Tewari and McLean (1972) reported enthalpies and entropies for the transfer of potential determining ions from bulk solution to the surface of various oxides including magnetite. The general observation is that the point of zero charge shifts towards lower values as the temperature increases in the studied temperature range, 25 °C–90 °C. Based on a thermodynamic analysis of the double layer, Bérubé and de Bruyn (1968) derived equations and determined numerical values for the enthalpy and entropy changes accompanying the process

$$\equiv M\text{–}O^- + H_2O + H^+ = \equiv M\text{–}OH_2^+ + OH^- \qquad (60)$$

which is equivalent to the transfer of 1 mole of protons from the bulk to the interface plus the transfer of 1 mole of hydroxide ions from the interface to the bulk solution.

Lyklema and coworkers (Lyklema 1987; Fokkink et al. 1989) presented a more rigorous and general relation between an adsorption enthalpy and the shift of the point of zero charge. By considering the charge formation process as solely due to adsorption and desorption of protons, they derived a variant of the van´t Hoff equation enabling the calculation of the adsorption enthalpy of protons. By plotting the obtained $pH_{pzc}$ values for rutile and hematite as a function of inverse temperature in the temperature range studied (5 °C–60 °C), the molar enthalpy change of proton adsorption at the point of zero charge could be determined from the slopes of the curves. Further, they gave equations relating their parameters to those extracted by Bérubé and de Bruyn (1968).

## 5.2 Calorimetric studies

Two studies employing calorimetric titrations to measure the heat changes accompanying adsorption processes on iron oxides were found. Machesky and Anderson (1986) used this technique to study proton adsorption on goethite and rutile, while de Keizer et al. (1990) studied hematite and rutile. In spite of some experimental problems, e.g. exclusion of atmospheric carbon dioxide, calorimetric acid–base titrations are especially attractive, because free energy and enthalpy data can be obtained from the same sample. The heat involved in a reaction is measured as the adiabatic temperature change recorded with a thermistor. After calibration using a heating resistor, temperature changes can be directly converted into a total reaction enthalpy. Further, after correcting for various background effects, e.g. the enthalpies of the bulk neutralization reactions and dilution along with proton consumption due to solution reactions, the end results are moles of $H^+$ adsorbed on the solid and the corresponding heat change. de Keizer et al. (1990) compared their calorimetric results on both minerals to those obtained by the same group in a thermodynamic analysis of the shift in the point of zero charge with temperature (Lyklema 1987; Fokkink et al. 1989) and found a gratifying agreement. Machesky and Anderson (1986) combined the calorimetric data with acid–base modelling results (using the constant capacitance model) and discussed the trends in the thermodynamic functions; free energy, entropy and enthalpy.

## 5.3 Determination of equilibrium constants at various ambient temperatures

Although Lyklema and coworkers (Lyklema 1987; Fokkink et al. 1989) refrained from the use of surface complexation models in their thermodynamic analysis, their description is compatible with such models as pointed out by Blesa et al. (1990), who were the first to describe the influence of temperature on the whole surface charge vs. pH profile in terms of the triple layer model (Blesa et al. 1984). They conducted potentiometric acid–base titrations with magnetite suspensions at 30 °C, 50 °C and 80 °C at different concentrations of $KNO_3$. In addition to evaluation of the temperature dependence of the point of zero charge, they determined the values of the four equilibrium constants of the triple-layer model (the intrinsic acid dissociation constants, $\mathrm{p}K_{\mathrm{a1}}^{\mathrm{int}}$ and $\mathrm{p}K_{\mathrm{a2}}^{\mathrm{int}}$, and the intrinsic constants for the binding of $NO_3^-$ and $K^+$, $\mathrm{p}K_{\mathrm{anion}}^{\mathrm{int}}$ and $\mathrm{p}K_{\mathrm{cation}}^{\mathrm{int}}$) and the inner-layer capacitance $C_1$, at each temperature. All four $K^{\mathrm{int}}$ values increase with increasing temperature and the corresponding enthalpy and entropy changes were obtained from $\mathrm{p}K^{\mathrm{int}}$ vs. $T^{-1}$ plots. The determined enthalpy and entropy values of the acid dissociation reactions were also related to the parameters of Lyklema and coworkers. A similar approach in the cases of hematite and goethite has been recently taken by Karasyova et al. (1999) and Angove et al. (1999), who, however, employed the constant capacitance model while interpreting the results.

## 5.4 Potentiometric acid–base titrations at high temperatures and pressures

Potentiometric titrations at high temperatures and pressures (i.e. over 100 °C) are starting to be applied for studying adsorption on mineral surfaces. Until now, however, only one research group has been able to conduct such measurements, and results on two minerals, rutile and magnetite, are available (Machesky et al. 1994, 1998a, 1998b; Ridley 1999; Wesolowski et al. 2000). In their first published work, hydrogen ion adsorption on rutile surfaces in NaCl media (0.01–1.0 *m*) between 25 °C and 250 °C was determined using a stirred hydrogen-electrode concentration cell located at Oak

Ridge National Laboratory (Machesky et al. 1994). In a subsequent paper, published four years later, the experimental data, acquired over a wide range of temperatures (25 to 250 °C) and ionic strengths (0.03 to 1.1 *m*), was interpreted by means of a one-p*K* three-layer surface complexation model (Machesky et al. 1998a). In this model, the surface protonation constant (log $K_H$) can be equated with the $pH_{ppzc}$, which in the case of rutile provides a formal link to the the thermodynamic analysis of the temperature dependence of the observed $pH_{cip}$ values assumed to be equal to the $pH_{ppzc}$ values. As a result of a thermodynamic analysis and data fitting procedure, the standard enthalpy, entropy and heat capacity changes associated with proton adsorption were determined.

In an extensive paper that has just come out, the Oak Ridge research group has applied the same methodology in an investigation of proton-induced surface charge of magnetite in 0.03 *m* and 0.30 *m* sodiumtrifluoromethanesulfonate solutions in the temperature range of 25 °C to 290 °C and at pHs spanning from mildly acidic to strongly basic conditions (Wesolowski et al. 2000). Compared to rutile, magnetite is relatively reactive (soluble, redox reactive) impeding the interpretation of the experimental results. As a consequence, the experimentally observed $pH_{cip}$ values were suspect to be influenced by dissolution artifacts. Further, the modelling efforts employing the one-p*K* model indicated a strong specific binding of $Na^+$. Because of these effects, the $pH_{cip}$ was not taken as the pristine point of zero charge, which, instead, was approximated as the inflection point ($pH_{infl}$) observed in the proton sorption isotherms at a somewhat higher pH than the $pH_{cip}$. By equating the $pH_{infl}$ values to the one-p*K* protonation constant and fitting them to a temperature function, Wesolowski et al. (2000) derived the thermodynamic quantities of the protonation reaction on magnetite in a similar way as they did for rutile. In both cases, the surface protonation reaction associated with the one-p*K* model exhibits a negative enthalpy and a large positive heat capacity of reaction.

## 5.5 Surface complexation of metals on iron oxides at elevated temperatures

In a recent paper, Angove et al. (1999) studied the adsorption of cobalt and cadmium on goethite at five temperatures between 10 °C and 70 °C performing three different types of experiment; 1) potentiometric titrations of goethite suspensions in the presence and absence of added cation, 2) adsorption edge measurements and 3) adsorption isotherm measurements at constant pH. It should be pointed out that, even the first kind of experiments would be enough to determine adsorption. Protons are released as cations sorb, so that titration curves are shifted to lower pH values. As a result, they presented a constant capacitance surface complexation model which, in addition to the acid–base reactions (1) and (2), assumed the adsorption reactions

$$Co^{2+} + \equiv Fe–OH = \equiv Fe–OCo^{+} + H^{+} \qquad (61)$$

$$Co^{2+} + \equiv Fe–OH + H_2O = \equiv Fe–OCoOH + 2H^{+} \qquad (62)$$

and was consistent with all three types of experimental data. From the temperature dependence of the fitted equilibrium constants they determined the entropies and enthalpies of the surface reactions in a standard way utilizing the van´t Hoff equation.

They modelled the adsorption isotherm data also with the Langmuir isotherm which makes no attempt to detail the particular reactions that occur during adsorption, but presents the overall process simply as

$$Co(aq) + \equiv Fe(surf) = \equiv Fe(surf)–Co \qquad (63)$$

where Co(aq) denotes any soluble form of cobalt, ≡Fe(surf) a surface site, and ≡Fe(surf)-Co adsorbed cobalt in any form. "Equilibrium constants" are also derived in this approach, but unlike those of surface complexation models, they represent multiple reactions rather than specific surface reactions. Overall adsorption enthalpies and entropies were determined from the temperature dependence of the Langmuirian equilibrium constants as well. As the adsorption system in these approaches is defined in quite different ways, the thermodynamic parameters cannot be easily compared. However, both models showed that the adsorption was endothermic, the amount of cobalt adsorbing on goethite surface increasing when the temperature increased.

A similar surface complexation approach was recently taken by Karasyova et al. (1999) who studied strontium adsorption on hematite at three different temperatures (25 °C, 50 °C and 75 °C) employing precise potentiometric titrations supplemented by AAS analyses of Sr in the solution. The combined effect of the $pH_{pzc}$ decrease and the positive enthalpies of surface complex formation was found to favour dramatically strontium adsorption at the hematite surface at enhanced temperatures.

A kind of surface complexation approach was also taken by Tamura et al. (1983), who investigated the adsorption of $Co^{2+}$ on spherical magnetite particles at the temperature range of 25 °C–75 °C and explained the results by considering the formation of two kinds of surface complexes according to reactions (64) and (65).

$$Co^{2+} + \equiv FeOH = \equiv FeOCo^{+} + H^{+} \qquad (64)$$

$$Co^{2+} + 2\equiv FeOH = \equiv (FeO)_2Co + 2H^{+} \qquad (65)$$

Although considering complexation on surface sites, they did not take the electrostatic interaction between metal ions in solution and solid surfaces into account in the standard way ($\Delta G_{\mathrm{elect}} = \Delta ZF\psi$), but derivated equations relating the apparent equilibrium constants to surface coverage and intrinsic equilibrium constants. From the temperature dependence of the intrinsic equilibrium constants, enthalpy and entropy values for reactions (64) and (65) were determined.

Several researchers have taken the Langmuirian and related approaches in order to explain the effect of temperature on zinc and cobalt adsorption on iron oxides. Srivastava and Srivastava (1990) measured zinc adsorption on ferrihydrite at 15 °C and 35 °C and Rodda et al. (1993, 1996) on goethite between 10 °C and 70 °C. Cobalt adsorption on magnetite at the temperature range of 30 °C to 100 °C was studied by Tewari et al. (1972), while Karasawa et al. (1986, 1987) extended the temperature range and found the equilibrium constant describing cobalt adsorption on hematite to increase 570 fold as the temperature increased from 20 °C to 285 °C.

Although not dealing with iron oxides, the recent paper on calcium adsorption on rutile by Ridley et al. (1999) should be mentioned. This is the first work combining metal uptake and proton release measurements under the hydrothermal regime. Using the hydrogen-electrode concentration cell, they monitored the net proton adsorption in the presence and absence of $Ca^{2+}$ at the temperature range of 25 °C–250 °C, and supplemented the data by withdrawing samples for $Ca^{2+}$ analysis. The results have not yet been interpreted by means of a surface complexation model, but adsorption increased with temperature and the constant (with respect to temperature) proton release value of ca 1.5 protons per one adsorbed calcium suggests that the adsorption mechanism does not change with temperature. Although not dealing with iron oxides, this paper by Ridley et al. (1999) along with the above mentioned other papers by the Oak Ridge research group is of great importance also for the present problem showing promise that potentiometric titrations of iron oxide suspension can be extended into the high-temperature, high-pressure regime.

## 5.6 Conclusions of temperature-dependent studies on surface complexation on iron oxides

Until recent past, the focus of the studies was on the acid–base properties of the iron oxides and especially on the temperature dependence of the point of zero charge. Although necessary, this is only one piece of information that is needed to evaluate the adsorption behaviour at elevated temperatures. To properly evaluate the importance of adsorption, it is necessary to know the effect of temperature on a broad range of solution and surface complexation reactions. In addition to various surface complexation models, more empirical approaches involving the use of Langmuir or similar equations have been used in interpreting the effect of temperature in studies concerning adsorption of zinc and cobalt on iron oxides. These models assume different sorption reactions and treat the interaction between the adsorbing species and the surface in different ways generating different equilibrium constants along with associated enthalpy and entropy values.

Although a quantitative evaluation of the published thermodynamic values and the selection of the most suitable model system for our purposes will be done in a subsequent report, a few general conclusions are drawn from the studies considered above.

At elevated temperatures, the charging of the oxide surface will play a much more significant role in the adsorption of ions than at 25 °C.Increasing the temperature of the system promotes significantly cation uptake.

The $pH_{ppzc}$ of oxides decreases with increasing temperature to 200 °C. In the case of experimentally studied rutile and magnetite, the $pH_{ppzc}$ became relatively independent of temperature between 200 °C and 300 °C.

For a given pH above the point of zero charge, the surface charge density increases significantly with increasing temperature.

These general trends emphasize the need of a proper surface complexation model for understanding and predicting adsorption phenomena at elevated temperatures prevailing in the primary circuits of nuclear power plants.

# 6. Summary

The interaction between the construction materials of nuclear power plants and the aqueous coolant leads to the formation of oxide films on the piping surfaces and to the release of small amounts of metals, e.g. $^{59}$Co, into the coolant. The released cobalt is carried by the coolant into the core of the nuclear reactor where the $^{60}$Co isotope is formed by neutron activation of the natural cobalt. Finally, the activated species are redistributed in the cooling circuit and subsequently deposited on the system surfaces which are exposed to reactor water. This activity transport and buildup of radiation fields may result in increased occupational doses of radiation for the personnel of the plant. A novel method to decrease the incorporation of $^{60}$Co is injection of zinc into the primary coolant. Although the exact mechanisms by which zinc affects are not known, the fundamental assumption in this work is that the first step of the incorporation process is adsorption and that the competitive adsorption of zinc and cobalt can be modelled using the surface complexation approach.

Despite the uncertainty in the exact composition and structure of the iron oxide film formed on the material surfaces, it is evident that the hydrated passive film on iron and steels displays the coordinative properties of the Fe(lll) surface hydroxyl groups, ≡Fe–OH. These groups are ampholytes being able to react as follows:

$$\equiv\text{Fe–OH} + \text{H}^+ = \equiv\text{Fe–OH}_2^+ \qquad (66)$$

$$\equiv\text{Fe–OH} = \equiv\text{Fe–O}^- + \text{H}^+ \qquad (67)$$

By considering the Lewis base behaviour of the deprotonated surface hydroxyls, metal adsorption can be described by various surface complex formation reactions, e.g.

$$\equiv\text{FeOH} + \text{Co}^{2+} = \equiv\text{FeOCo}^+ + \text{H}^+ \qquad (68)$$

$$\equiv\text{FeOH} + \text{Zn}^{2+} = \equiv\text{FeOZn}^+ + \text{H}^+ \qquad (69)$$

By considering reactions (66–69), it is obvious that the net surface charge changes as the reactions advance resulting in a variable electrostatic energy of interaction between the surface site and the reacting solute. Models which combine chemical descriptions such as reactions (66–69) of the surface hydroxyl group and coulombic corrections based on an assumed electrical double layer structure are termed surface complexation models. Three of the most common surface complexation models are the constant capacitance model, the diffuse layer model and the triple layer model differing principally in the number of considered separate layers at the oxide–solution interface and, consequently, in the location of various adsorbing species. As a consequence, the electrostatic equations which are used to relate surface potential to surface charge, i.e., the way free energy of adsorption is divided into its chemical and electrostatic components, are different for each model. The output of a surface complexation model is a set of postulated surface reactions with associated equilibrium constants which can be combined with a conventional equilibrium model for the solution chemistry to predict adsorption in systems outside those studied.

Surface complexation models are becoming increasingly popular in describing adsorption phenomena, probably because they propose specific surface reactions and at the same time can take into account complex solution chemistry. The selection of the surface reactions is guided by theoretical considerations, chemists´ intuition, and spectroscopic measurements (to some extent) and substantiated by a successful fit of the data consisting of acid–base titration curves, adsorption edges and adsorption isotherms. Although a particular set of reactions along with a particular implementation of the associated electrostatic aspects may describe the macroscopic behaviour of the system closely, this, per se, is no guarantee that those reactions actually occur. In fact, in many cases existing data has been interpreted with a variety of surface complexation models which are not consistent with each other. The situation can be summarized by emphasizing that the chemical species defined and the equilibrium constants obtained with one model must never be used as such in any other model.

In this study we assumed the very outermost layer of the oxide film to be more or less hydrated and poorly ordered resembling ferrihydrite known also as hydrous ferric oxide. In the case of this sorbent, a coherent compendium of self-consistent surface complexation constants valid at 25 °C and based on a generalized diffuse layer model are available in the literature. Combining this information for reactions (66–69) with the known solution complexation reactions and the knowledge of the actual cooling system (the physical properties of the system and the chemical composition of the coolant), the adsorption behaviour of zinc and cobalt can be estimated using computer programs developed for chemical equilibrium calculations. The calculations carried out in this work by the HYDRAQL modelling software show that the surface complexation approach correctly predicts the retarding effect of zinc on the cobalt adsorption on ferrihydrite at 25 °C under conditions otherwise relevant to those prevailing in the cooling systems of nuclear power plants. For example, we simulated the effect of decreasing the dissolved zinc concentration from 0.2 ppb to 0.02 ppb resembling the changes observed in some BWR coolants. Due to this decrease in the dissolved zinc concentration, the adsorbed amount of cobalt in equilibrium with a dissolved cobalt concentration of 0.03 ppb is more than doubled.

Despite the importance of temperature on adsorption, studies at other than room temperature are rare, and the pioneering surface complexation studies at temperatures above 100 °C have been published in the recent past. The few studies in this field indicate that at elevated temperatures, the charging of the oxide surface plays a much more significant role in the adsorption of ions than at room temperature. Increasing the temperature of the system has been found to promote significantly cation uptake. For example, in the case of cobalt adsorption on magnetite an increase of two orders of magnitude was observed as the temperature increased from 20 °C to 285 °C.

Although incorporation of activated $^{60}$Co species in the oxide films formed on material surfaces in the primary circuits in nuclear power plants is a complicated process involving several steps, this study reveals that it is possible to model the first step of this incorporation employing the surface complexation approach. The experimentally observed retarding effect of zinc addition on cobalt incorporation can be quantitatively understood by means of competitive surface complexation. Two general trends, the decrease of the point of zero charge and the positive enthalpies of cation surface complexation, emphasize the importance of surface complexation in understanding cation adsorption at the elevated temperatures prevailing in the primary circuits. However, quantitative modelling of adsorption phenomena at elevated temperatures in terms of the surface complexation models requires information on the temperature dependence of the equilibrium constants of the surface and solution reactions. Finding and assessing this data will be one of the main tasks during the rest of this subproject.

# Acknowledgements

The authors are grateful to the Radiation and Nuclear Safety Authority, Finland, and to the Finnish Ministry of Trade and Industry for the financial support of this work in terms of the Research Programme on Operational Safety and Structural Integrity 1999–2002, FINNUS. Mr Juhani Hinttala (M.Sc. Tech.) is acknowledged for supervising this work on the behalf of the Radiation and Nuclear Safety Authority.

# References

Angove, M., Wells, J. & Johnson B., 1999. The influence of temperature on the adsorption of cadmium (ll) and cobalt (ll) on goethite, Journal of Colloid and Interface Science Vol. 211, pp. 281–290.

Bard, A. & Faulkner, L. 1980. Electrochemical methods, Fundamentals and applications. New York: John Wiley & Sons. 718 pp.

Barrow, N. 1992. A brief discussion on the effect of temperature on the reaction of inorganic ions with soil. Journal of Soil Science, Vol. 43, pp. 37–45.

Benjamin, M. M. 1978. Effects of competing metals and complexing ligands on trace metal adsorption at the oxide/solution interface. Ph.D. Thesis, Stanford University, Stanford, CA.

Benjamin, M. & Bloom, N. 1981. Effects of strong binding adsorbates on adsorption of trace metals on amorphous iron oxyhydroxide. In: Tewari P. (Ed.) Adsorption from aqueous solutions. New York: Plenum Press. Pp. 41–60.

Benjamin, M. & Leckie, J. 1981. Competitive adsorption Cd, Zn, Cu and Pb on amorphous iron oxyhydroxide. Journal of Colloid and Interface Science Vol. 83, pp. 410–419.

Bérubé, Y. & de Bruyn, P. 1968. Adsorption at the rutile–solution interface, Thermodynamic and experimental study. Journal of Colloid and Interface Science, Vol. 28 pp. 305–318.

Beverskog, B., Bojinov, M., Kinnunen, P., Laitinen, T., Mäkelä, K., Saario, T. & Sirkiä, P. 2000a. A mixed conduction model for anodic oxide films on Fe, Cr and Fe–Cr alloys at high temperatures, I. Comparison of the electrochemical behaviour at room temperature and at 200 °C. Submitted to Corrosion Science.

Beverskog, B., Bojinov, M., Kinnunen, P., Laitinen, T., Mäkelä, K. & Saario, T. 2000b. A mixed conduction model for anodic oxide films on Fe, Cr and Fe-Cr alloys at high temperatures, II. Adaptation and justification of the model. Submitted to Corrosion Science.

Blesa, A., Figliolia, N., Maroto, A. & Regazzoni, A. 1984. The influence of temperature on the interface magnetite–aqueous electrolyte solution. Journal of Colloid and Interface Science, Vol. 101, pp. 410–418.

Blesa, M., Maroto, A. & Regazzoni, A. 1990. Surface acidity of metal oxides immersed in water: A critical analysis of thermodynamic data. Journal of Colloid and Interface Science, Vol. 140, pp. 287–290.

Bojinov, M., Fabricius, G., Laitinen, T., Mäkelä, K., Saario, T. & Sundholm G. 2000a. Coupling between ionic defect structure and electronic conduction in passive films on iron, chromium and iron-chromium alloys. Electrochimica Acta Vol. 45, pp. 2029–2048.

Bojinov, M., Fabricius, G., Laitinen, T., Mäkelä, K., Saario, T. & Sirkiä, P. 2000b. Electrical and electrochemical properties of the passive films on stainless steels in neutral solution at ambient and elevated temperature. In: Ives, M. B., Luo, J. L. & Rodda J. (Eds.). Passivity of metals and semiconductors. Pennington, NJ: The Electrochemical Society. Pp. 201–207. (Proceedings of the 8th International Symposium.)

Bojinov, M., Laitinen, T., Mäkelä, K. & Saario, T. 200c. A conduction mechanism of the passive film on iron based on contact electric impedance and resistance measurements. Submitted to Journal of the Electrochemical Society.

Brown, G., Henrich, V., Casey, W., Clark, D., Eggleston, C., Felmy, A., Goodman, D., Grätzel, M., Maciel, G., McCarthy, M., Nealson, K., Sverjensky, D., Toney, M. & Zachara, J. 1999. Metal oxide surfaces and their interactions with aqueous solutions and microbial organisms. Chemical Reviews, Vol. 99, pp. 77–174.

Cornell, R. & Schwertmann, U. 1996. The Iron Oxides, Structure, properties, reactions, occurrence and uses. Weinheim: VCH. 537 pp.

Dempsey, B. & Singer, P. 1980. The effects of calsium on the adsorption of zinc by $MnO_x$(s) and $FeOH_3$(am). In: Baker, R. (Ed.) Contaminants and Sediments Vol. 2., Ann Arbor, MI: Ann Arbor Science. Pp. 333–352.

Duval, J. & Kurbatov, M. 1952. The adsorption of cobalt and barium ions by hydrous ferric oxide at equilibrium. Journal of Physical Chemistry, Vol. 56, pp. 982–984.

Dzombak, D. & Morel, F. 1990. Surface complexation modeling, Hydrous ferric oxide. New York: John Wiley & Sons. 393 pp.

Fokkink, L., de Keizer, A. & Lyklema, J. 1989. Temperature dependence of the electrical double layer on oxides: Rutile and hematite. Journal of Colloid and Interface Science, Vol. 127, pp. 116–131.

Fornasiero, D., Eijt, V. & Ralston, J. 1992. An electrokinetic study of pyrite oxidation, Colloids and Surfaces, Vol. 62, pp. 63–73.

Goldberg, S. 1992. Use of surface complexation models in soil chemical systems. In: Sparks, D. (Ed.) Advances in agronomy, Vol. 47. San Diego, CA: Academic Press. pp. 234–329.

Hamann, C. & Vielstich, W. 1985. Electrochemie l, Elektrolytische Leitfähigkeit, Potentiale, Phasengrenzen, 2. überarbeitete Auflage. Weinheim: VCH Verlags-gesellschaft.

Hayes, K. 1987. Equilibrium, spectroscopic, and kinetic studies of ion adsorption at the oxide/aqueous interface. Ph.D. thesis, Stanford University, Department of Civil Engineering, Stanford, CA.

Hayes, K. & Katz, L. 1996. Application of X-ray absorption spectroscopy for surface complexation modeling of metal ion sorption. In: Brady, P. (Ed.) Physics and chemistry of mineral surfaces. Boca Raton, FL: CRC Press. Pp. 147–223.

Hayes, K. & Leckie, J. 1987. Modeling ionic strength effects on cation adsorption at hydrous oxide/solution interfaces. Journal of Colloid and Interface Science, Vol. 115, pp. 564–572.

Herbelin, A. & Westall, J. 1999. FITEQL, A computer program for determination of chemical equilibrium constants from experimental data, Version 4.0. Corvallis, OR: Oregon State University, Department of Chemistry. (Report 99-01).

Huang, C. & Stumm, W. 1973. Specific adsorption of cations on hydrous $\gamma$-$Al_2O_3$, Journal of Colloid and Interface Science, Vol. 43, pp. 409–420.

IUPAC (International Union of Pure and Applied Chemistry), Division of physical chemistry 1972. Manual of symbols and terminology for physicochemical quantities and units, Appendix ll, Definitions, terminology and symbols in colloid and surface chemistry, Part l. Prepared for publication by D. H. Everett. Pure and Applied Chemistry, Vol. 31, pp. 577–638.

IUPAC (International Union of Pure and Applied Chemistry), Physical chemistry division, Commission on electrochemistry 1983. Interphases in systems of conducting phases, Provisional recommendations prepared for publication by S. Trasatti and R. Parsons. Pure and Applied Chemistry, Vol. 55, pp. 1251–1268.

James, R., Stiglich, P. & Healy, T. 1975. Analysis of models of adsorption of metal ions at oxide/water interfaces, Faraday Discussions of the Chemical Society, Vol. 59, pp. 142–156.

Jenne, E. 1998. Adsorption of metals by geomedia: Data analysis, modeling, controlling factors, and related issues. In: Jenne, E. (Ed.) Adsorption of metals by geomedia, Variables, mechanisms and model applications. San Diego, CA: Academic Press. Pp. 1–73.

Karasawa, H., Yamato, A., Masaharu, S. & Shunsuke, U. 1987. Experimental evaluation of cobalt behavior on BWR fuel rod surface. In: Corrosion 87. Moscone Center, San Francisco, CA. Paper number 81.

Karasawa, H., Yamato, A., Masaharu, S. & Shunsuke U. 1986. Adsorption of cobalt ions on hematite particles. Journal of Nuclear Science and Technology, Vol. 23, pp. 926–927.

Karasyova, O., Ivanova, L., Lakshtanov, L. & Lövgren, L. 1999. Strontium sorption on hematite at elevated temperatures. Journal of Colloid and Interface Science, Vol. 220, pp. 419–428.

Keizer, A. de, Fokkink, L. & Lyklema, J. 1990. Thermodynamics of proton charge formation on oxides, Microcalorimetry. Colloids and Surfaces, Vol. 49, pp. 149–163.

Kinniburgh, D. & Jackson, M. 1982. Concentration and pH dependence of calcium and zinc adsorption by iron hydrous oxide gel. Soil Science Society of America, Journal, Vol. 46, pp. 56–61.

Kinniburgh, D., Sridhar, K. & Jackson, M. 1977. Specific adsorption of zinc and cadmium by iron and aluminum hydrous oxides. In: Proceedings of the 15th Hanford Life Sciences Symposium on Biological Implications of Metals in the Environment. Hanford, WA. Pp. 231–239.

Kinniburgh, D. 1983. The $H^+/M^{2+}$ exchange stoichiometry of calcium and zinc adsorption by ferrihydrite. Journal of Soil Science, Vol. 34, pp. 759–768.

Kurbatov, M., Wood, G. & Kurbatov, J. 1951. Isothermal adsorption of cobalt from dilute solutions. Journal of Physical Chemistry, Vol. 55, pp. 1170–1182.

Laitinen, T., Bojinov, M., Betova, I., Mäkelä, K. & Saario, T. 1999. The properties of and transport phenomena in oxide films on iron, nickel, chromium and their alloys in aqueous environments. Helsinki: Radiation and nuclear safety authority (STUK). (Report STUK-YTO-TR 150)

Leckie, J., Benjamin, M., Hayes, K., Kaufman G. & Altman, S. 1980. Adsorption/Coprecipitation of trace elements from water with iron oxyhydroxide. Palo Alto, CA: Electric Power Research Institute. (Report RP-910-1)

Lehikoinen, J. & Olin, M. 2000. Modelling the transport in the porous layer of oxide films formed on material surfaces in nuclear power plants. - A BWR case study. Espoo: VTT. (VTT Research Notes)

Lyklema, J. 1987. Electrical double layers on oxides; disparate observations and unifying principles. Chemistry and Industry, pp. 741–747.

Machesky, M. 1990. Influence of temperature on ion adsorption by hydrous metal oxides. In: Melchior, D. & Bassett, R. (Eds.) Chemical Modeling in Aqueous systems ll. Washington, DC: American Chemical Society. Pp. 282–292. (ACS Symp. Ser., Vol. 416)

Machesky, M. & Anderson, M. 1986. Calorimetric acid–base titrations of aqueous goethite and rutile suspensions. Langmuir, Vol. 2, pp. 582–587.

Machesky, M., Palmer, D., & Wesolowski, D. 1994. Hydrogen ion adsorption at the rutile–water interface to 250 °C. Geochimica Cosmochimica Acta, Vol. 58, pp. 5627–5632.

Machesky, M., Wesolowski, D., Palmer, D. & Ichiro-Hayashi, K. 1998a. Potentiometric titrations of rutile suspensions to 250 °C. Journal of Colloid and Interface Science, Vol. 200, pp. 298–309.

Machesky, M., Ridley, M., Wesolowski, D. & Palmer, D. 1998b. Ion adsorption by metal oxides under hydrothermal conditions. Mineralogical Magazine and Journal of the Mineralogical Society 62A(Pt. 2), pp. 935–936.

McKenzie, R. M. 1980. The adsorption of lead and other heavy metals on oxides of manganese and iron. Australian Journal of Soil Research, Vol. 18, pp. 61–73.

Morel, F. & Hering, J. 1993. Principles and applications of aquatic chemistry. New York: John Wiley & Sons. 588 pp.

Mäkelä, K, Laitinen, T. & Bojinov, M. 1999. The influence of modified water chemistries on metal oxide films, activity build-up and stress corrosion cracking of structural materials in nuclear power plants. Helsinki: Radiation and nuclear safety authority (STUK). (Report STUK-YTO-TR 152)

Palmqvist, U., Ahlberg, E., Lövgren, L. & Sjöberg, S. 1999. Competitive metal ion adsorption in goethite systems using in situ voltammetric methods and potentiometry. Journal of Colloid and Interface Science, Vol. 218, pp. 388–396.

Papelis, C., Hayes, K. F. & Leckie, J. O., 1988. HYDRAQL: A program for the computation of chemical equilibrium composition of aqueous batch systems including surface complexation modeling of ion adsorption at the oxide/solution interface. Stanford, CA: Stanfors University, Department of civil engineering. (Technical report n:o 306).

Ridley, M., Machesky, M., Wesolowski, D. & Palmer, D. 1999. Calcium adsorption at the rutile-water interface: a potentiometric study in NaCl media to 250 °C. Geochimica et Cosmochimica Acta, Vol. 63, pp. 3087–3096.

Rodda, D., Johnson, B. & Wells, J. 1993. The effect of temperature and pH on the adsorption of copper(ll), lead(ll) and zinc(ll) onto goethite. Journal of Colloid and Interface Science, Vol. 161, pp. 57–62.

Rodda, D., Johnson, B. & Wells, J. 1996. Modelling the effect of temperature on adsorption of lead(ll) and zinc(ll) onto goethite at constant pH. Journal of Colloid and Interface Science, Vol. 184, pp. 365–377.

Schindler, P. 1981. Surface complexes at oxide–water interfaces. In: Anderson, M. & Rubin, A. (Eds.) Adsorption of inorganics at solid–liquid interfaces. Ann Arbor, MI: Ann Arbor Science. Pp. 1–49.

Schindler, P. & Gamsjäger, H. 1972. Acid–base reactions of the $TiO_2$ (Anatase)–water interface and the point of zero charge of $TiO_2$ suspensions, Kolloid-Zeitschrift und Zeitschrift für Polymere, Vol. 250, pp. 759–763.

Schindler, P. & Kamber, H. 1968. Die Acidität von Silanolgruppen, Helv. Chim. Acta, Vol. 51, pp. 1781–1786.

Schindler, P. & Stumm, W. 1987. The surface chemistry of oxides, hydroxides, and oxide minerals. In: Stumm, W. (Ed.) Aquatic surface chemistry, Chemical processes at the particle–water interface. New York: John Wiley & Sons. Pp. 83–110.

Schoonen, M. 1994. Calculation of the point of zero charge of metal oxides between 0 °C and 350 °C. Geochimica et Cosmochimica Acta, Vol. 57, pp. 2845–2851.

Smith, K., Ranville, J., Plumlee, G. & Macalady, D. 1998. Predictive double layer modelling of metal sorption in mine-drainage systems. In: Jenne, E. (Ed.) Adsorption of metals by geomedia, Variables, mechanisms and model applications. San Diego, CA: Academic Press. Pp. 521–547.

Sipalo-Zulijevic, J. & Wolf, R. 1973. Sorption of lanthanum(lll), cobalt(ll) and iodide ions at trace concentrations on ferric hydroxide. Mikrochimica Acta, pp. 315–320.

Sposito, G. 1984. The surface chemistry of soils. New York: Oxford University Press. 234 pp.

Srivastava, A. & Srivastava, P. 1990. Adsorption–desorption behaviour of zinc(ll) at iron hydroxide–aqueous solution interface as influenced by pH and temperature. Environmental Pollution, Vol. 68, pp. 171–180.

Stumm, W. 1995. The inner-sphere surface complex, A key to understanding surface reactivity. In: Huang, C., O´Melia, C. & Morgan, J. (Eds.) Aquatic chemistry, Interfacial and Interspecies Processes. Washington DC: American Chemical Society. Pp. 1–32. (Advances in chemistry series, Vol. 244)

Stumm, W. 1992. Chemistry of the solid–water interface, Processes at the mineral–water and particle–water interface in natural system. New York: John Wiley & Sons. 428 pp.

Stumm, W., Huang, C. & Jenkins, S. 1970. Specific chemical interaction affecting the stability of dispersed systems. Croatica Chemica Acta, Vol. 42, pp. 223–245.

Stumm, W. & Morgan, J. 1981. Aquatic chemistry, An introduction emphasizing chemical equilibria in natural waters, 2nd ed. New York.: John Wiley & Sons. 780 pp.

Tamura, H., Matijevic, E. & Meites, L. 1983. Adsorption of $Co^{2+}$ ions on spherical magnetite particles. Journal of Colloid and Interface Science, Vol. 92, pp. 303–314.

Tewari, P., Campbell, A. & Lee, W. 1972. Adsorption of $Co^{2+}$ by oxides from aqueous solution. Canadian Journal of Chemistry, Vol. 50, pp. 1642–1648.

Tewari, P. & McLean, A. 1972. Temperature dependence of point of zero charge of alumina and magnetite. Journal of Colloid and Interface Science, Vol. 40, pp. 267–272.

Wesolowski, D., Machesky, M., Palmer, D. & Anovitz, L. 2000. Magnetite surface charge studies to 290 °C from in situ pH titrations. Chemical Geology, Vol. 167, pp. 193–229.

Westall, J. 1980. Chemical equilibrium including adsorption on charged surfaces. In: Kavanaugh, M. & Leckie, J. (Eds.) Particulates in water, Characterization, fate, effects, and removal. Washington DC: American Chemical Society. Pp. 33–44. (ACS Advances in chemistry series, Vol. 189)

Westall, J. 1982. FITEQL, A computer program for determination of chemical equilibrium constants from experimental data. Corvallis, OR: Oregon State University, Department of Chemistry. (Technical reports 82-01 (version 1.2) and 82-02 (version 2.0))

Westall, J. 1986. Reactions at the oxide–solution interface: Chemical and electrostatic models. In: Davis, J. & Hayes. K. (Eds.) Geochemical processes at mineral surfaces. Washington DC: American Chemical Society. Pp. 54–78. (ACS Symposium Series, Vol. 323)

Westall, J. 1987. Adsorption mechanisms in aquatic surface chemistry. In: Stumm, W. (Ed.) Aquatic surface chemistry. New York: Wiley, pp. 3–32.

Westall, J. & Hohl, H. 1980. A comparison of electrostatic models for the oxide/solution interface, Advances in Colloid and Interface Science, Vol. 12, pp. 265–294.

Wood, R., Fornasiero, D. & Ralston, J. 1990. Electrochemistry of the boehmite–water interface. Colloids and Surfaces, Vol. 51, pp. 389–403.

Yates, D., Levine, S. & Healy, T. 1974. Site-binding model of the electrical double layer at the oxide/water interface, Journal of the Chemical Society, Faraday Transactions 1, Vol. 70, pp. 1807–1818.

Zhang, Q., Xu, Z. & Finch, J. 1995a. Surface ionization and complexation at the sphalerite/water interface. l. Computation of electrical double-layer properties of sphalerite in a simple electrolyte, Journal of Colloid and Interface Science, Vol. 169, pp. 414–421.

Zhang, Q., Xu, Z. & Finch, J. A. 1995b. Surface ionization and complexation at the sphalerite/water interface. ll. Computation of electrical double-layer properties of sphalerite in the presence of iron ions in a simple electrolyte, Journal of Colloid and Interface Science, Vol. 175, pp. 61–67.

Zhang, Q., Xu, Z. & Finch, J. 1995c. Prediction of species distribution at sphalerite / water interface, Minerals Engineering, Vol. 8, pp. 999–1007.

Published by

Vuorimiehentie 5, P.O.Box 2000, FIN-02044 VTT, Finland
Phone internat. +358 9 4561
Fax +358 9 456 4374

Series title, number and
report code of publication

VTT Research Notes 2055
VTT–TIED–2055

Author(s)

Stén, Pekka, Olin, Markus & Lehikoinen, Jarmo

Title

# Surface complexation on iron oxides with reference to the oxide films formed on material surfaces in nuclear power plants

Abstract

The construction materials used in coolant systems in nuclear power plants become covered with oxide films as a result of exposure to the aqueous coolant. The present work belongs to a research programme on the properties of such films and especially on the transport of inorganic species through the films. The focus is on the incorporation of the highly energetic long-lived cobalt isotope $^{60}$Co in the films causing build-up of radiation fields in the out-of-core system.

The first step in $^{60}$Co incorporation in the oxide films on the primary circuit surfaces is assumed to be adsorption which can be modelled using the surface complexation approach. The review begins with a general discussion of surface complexation on various iron oxides. After introducing the main concepts of surface complexation modelling, three of the most common models (the constant capacitance model, the diffuse layer model and the triple layer model) are discussed and compared.

The very outermost layer of the oxide film is assumed to be more or less hydrated and poorly ordered resembling ferrihydrite known also as hydrous ferric oxide. Consequently, the surface chemical properties of and adsorption on ferrihydrite are reviewed. Using the known and estimated physical properties of the cooling system, chemical composition of the coolant and literature data on the surface and solution reactions, equilibrium calculations are conducted by the HYDRAQL programme to predict adsorption behaviour of cobalt and zinc on ferrihydrite at 25 °C. Except temperature, the conditions simulated in these calculations are similar to those prevailing in the cooling systems. The calculations correctly predict the diminishing effect of zinc on cobalt adsorption.

The published surface complexation studies on iron oxides at elevated temperatures are reviewed. Despite the importance of the temperature on adsorption, surface complexation studies at other than room temperature are rare and the high-temperature, high-pressure regime is almost unexplored. The few studies found in the literature indicate that at the elevated temperatures, the charging of the oxide surface will play a much more significant role in the adsorption of ions than at room temperature. Increasing the temperature of the system is known to promote significantly cation uptake. Another general trend is the decrease of the point of zero charge of oxides with increasing temperature.

Keywords
nuclear power plants, adsorption, surface complexation, iron oxides, oxide films, ferrihydrite, hydrous ferric oxide, zinc, cobalt

Activity unit
VTT Chemical Technology, Mineral Processing, Tutkijankatu 1, P.O.Box 1405, FIN–83501 OUTOKUMPU, Finland

ISBN
951–38–5749-2 (soft back ed.)
951–38–5752–2 (URL: http://www.inf.vtt.fi/pdf/)

Project number
K9SU00195

Date
October 2000

Language
English, Finnish abstr.

Pages
70 p.

Price
B

Name of project
Modelling the adsorption and surface complexation of species at the film-solution interface

Commissioned by
Radiation and Nuclear Safety Authority, Finland;
Finnish Ministry of Trade and Industry KTM

Series title and ISSN
VTT Tiedotteita – Meddelanden – Research Notes
1235–0605 (soft back edition)
1455–0865 (URL: http://www.inf.vtt.fi/pdf/)

Sold by
VTT Information Service
P.O.Box 2000, FIN-02044 VTT, Finland
Phone internat. +358 9 456 4404
Fax +358 9 456 4374

Julkaisija

Vuorimiehentie 5, PL 2000, 02044 VTT
Puh. (09) 4561
Faksi (09) 456 4374

Julkaisun sarja, numero ja raporttikoodi

VTT Tiedotteita 2055
VTT–TIED–2055

Tekijä(t)

Stén, Pekka, Olin, Markus & Lehikoinen, Jarmo

Nimeke

# Pintakompleksaatio rautaoksideille, erityisesti ydinvoimalaitosten jäähdytysvesipiirien rakennemateriaalien oksidifilmeille

Tiivistelmä

Ydinvoimalaitosten jäähdytysvesipiirien putkistoissa käytettävien rakennemateriaalien pinnoille syntyy veden hapettavan vaikutuksen vuoksi hapettumakerros eli oksidifilmi. Tämä työ on osa näiden oksidifilmien ominaisuuksiin keskittyvää laajempaa tutkimuskokonaisuutta. Erityisen mielenkiinnon kohteena on radioaktiivisen koboltti-60-isotoopin joutuminen filmeihin, mikä aiheuttaa aktiivisuuden kerääntymistä primääripiirin pinnoille.

Tässä julkaisussa esitettävä tarkastelu perustuu oletukseen, jonka mukaan adsorptio filmi-jäähdytysvesirajapinnalla on ensimmäinen vaihe $^{60}$Co-isotoopin joutumisessa filmiin. Adsorptiota oksidipinnoille on 1970-luvulta lähtien kuvattu ns. pintakompleksaatiomallien avulla. Julkaisun alussa esitetään pintakompleksaatiomallinnuksen yleiset perusteet ja verrataan kolmea näissä malleissa tavallisimmin käytettyä tapaa kuvata ionisten osaslajien adsorptioon liittyvät sähköstaattiset vuorovaikutukset kiintoaine-liuosrajapinnoilla.

Rakennemateriaalien pinnoille korkealämpötilavedessä muodostuvien filmien uloimman kerroksen oletetaan tässä tarkastelussa muistuttavan huonosti kiteytynyttä raudan oksidia, ferrihydriittiä. Julkaisuun on koottu katsaus kirjallisuudessa esitetyistä ferrihydriitin pintakemiallisista ominaisuuksista sekä koboltin ja sinkin adsorptiota käsittelevistä tutkimuksista. Kirjallisuudesta haettujen pinta- ja liuosreaktioiden tasapainovakioiden sekä jäähdytysveden koostumuksesta ja järjestelmän fysikaalisista ominaisuuksista käytettävissä olevien tietojen perusteella on arvioitu sinkin ja koboltin adsorptiota oksidifilmeille. Laskut on tehty käyttäen HYDRAQL-ohjelmaa, jolla simuloidut olot lämpötilaa (25 °C) lukuun ottamatta, muistuttavat jäähdytysvesipiirien oloja. Laskentamalli ennustaa käytännössäkin havaitun jäähdytysveteen tapahtuvan sinkin lisäämisen koboltin adsorptiota vähentävän edullisen vaikutuksen.

Tärkeydestään huolimatta lämpötilan vaikutusta pintakompleksaatioon on tutkittu vain vähän. Korkealämpötilaoloissa (>100 °C) tutkimuksia on tehty vasta aivan viime vuosina ainoan tutkitun rautaoksidin ollessa magnetiitti. Lämpötilan vaikutus pintakompleksaatioon on kuitenkin merkittävä kationien adsorption kasvaessa huomattavasti lämpötilan noustessa. Toinen yleinen piirre on oksidien pinnan nollavarausta vastaavan pH:n pieneneminen lämpötilan kasvaessa.

Avainsanat

nuclear power plants, adsorption, surface complexation, iron oxides, oxide films, ferrihydrite, hydrous ferric oxide, zinc, cobalt

Toimintayksikkö

VTT Kemiantekniikka, Mineraalitekniikka, Tutkijankatu 1, PL 1405, 83501 OUTOKUMPU

| ISBN | Projektinumero |
|---|---|
| 951–38–5749-2 (nid.)<br>951–38–5752–2 (URL: http://www.inf.vtt.fi/pdf/) | K9SU00195 |

| Julkaisuaika | Kieli | Sivuja | Hinta |
|---|---|---|---|
| Lokakuu 2000 | engl., suom. tiiv. | 70 s. | B |

| Projektin nimi | Toimeksiantaja(t) |
|---|---|
| Modelling the adsorption and surface complexation of species at the film-solution interface | Säteilyturvakeskus, kauppa- ja teollisuusministeriö KTM |

| Avainnimeke ja ISSN | Myynti: |
|---|---|
| VTT Tiedotteita – Meddelanden – Research Notes<br>1235–0605 (nid.)<br>1455–0865 (URL: http://www.inf.vtt.fi/pdf/) | VTT Tietopalvelu<br>PL 2000, 02044 VTT<br>Puh. (09) 456 4404<br>Faksi (09) 456 4374 |